Geochimica et Cosmochimica Acta 369 (2024) 1–16

Contents lists available at ScienceDirect

Geochimica et Cosmochimica Acta

journal homepage: www.elsevier.com/locate/gca

Clumped isotope and $\Delta^{17}O$ measurements of carbonates in CM carbonaceous chondrites: New insights into parent body thermal and fluid evolution

Matthieu Clog [a,*], Paula Lindgren [b], Sevasti Modestou [c], Alex McDonald [a], Andrew Tait [a], Terry Donnelly [a], Darren Mark [a], Martin Lee [d]

[a] Scottish Universities Environmental Research Centre, Glasgow, United Kingdom
[b] Geological Survey of Sweden, Lund, Sweden
[c] University of Northumbria, Newcastle upon Tyne, United Kingdom
[d] School of Geographical and Earth Sciences, University of Glasgow, Glasgow, United Kingdom

ARTICLE INFO

Associate editor: Pierre Beck

Keywords:
CM chondrites
Clumped isotopes
Triple oxygen isotopes
Chondrite aqueous alteration
Chondrite parent body evolution

ABSTRACT

The CM carbonaceous chondrites are key archives for understanding the earliest history of the solar system. Their C-complex asteroid parent body(ies) underwent aqueous alteration, among the products of which are carbonate minerals that can faithfully record the conditions of their formation. In this study we report carbon, triple oxygen and clumped isotope compositions of carbonates in six CM chondrites which span a range in degrees of aqueous alteration (Allan Hills 83100, Cold Bokkeveld, LaPaz Icefield 031166, Lonewolf Nunataks 94101, Murchison, Scott Glacier 06043). $\Delta^{17}O$ values range from −2.6 to −1.0 ‰ (±0.1), and where calcite and dolomite co-exist their $\Delta^{17}O$ differ by 0.6 permil, suggesting precipitation from distinct fluids. Calculated crystallization temperatures range from 5 to 51 °C for calcite (typically ± 10 °C) and 75 to 101(±15) °C for dolomite. The $\delta^{18}O_{VSMOW}$ of the aqueous fluids from which they formed ranges from −6.6 to 2.3 ‰, with no relationship to the $\delta^{13}C$ of carbonates. As the population of carbonates in any one CM chondrite can include multiple generations of grains that formed at different conditions, these values represent the mode of the temperature of carbonate formation for each meteorite. We observe that in the more altered meteorites carbonate $\Delta^{17}O$ values are lower and formation temperatures are higher. These correlations are consistent with aqueous alteration of the CM chondrites being a prograde reaction whereby the hotter fluids had undergone greater isotope exchange with the anhydrous matrix. Our data are broadly consistent with the closed system model for water/rock interaction, but carbonate mineral formation in the latter stages of aqueous alteration may be linked to fluid movement via fractures.

1. Introduction

The Mighei-like (CM) carbonaceous chondrites are believed to sample one or more C-complex asteroids given similarities in their spectroscopic properties (Gradie & Tedesco, 1982; Burbine, 2016; Greenwood et al., 2020). Such an origin is also consistent with orbital data from the CM falls Maribo and Winchcombe (Borovička et al., 2019; King et al., 2022). These asteroidal parent body(ies) were built by the accretion of chondrules, refractory inclusions, individual mineral grains, particles of amorphous material including organic matter, and ices (DuFresne and Anders, 1962; Bunch and Chang, 1980; Tomeoka et al., 1989; Connolly et al., 2007). In addition to these primary constituents, nearly all CMs contain a suite of 'secondary' minerals that were produced by the aqueous alteration of parent body interiors. Products of these reactions are dominated by phyllosilicates (Mg,Fe serpentine, cronstedtite), with smaller proportions of sulphides (e.g., tochilinite, pentlandite), oxides (magnetite) and carbonates (e.g., calcite, dolomite) (Dufresne and Anders, 1962; Fuchs et al., 1973; Bunch and Chang, 1980; Barber, 1981; Mackinnon and Zolensky, 1984; Howard et al., 2015; Singerling and Brearley, 2018,2020). A subset of the CMs have undergone post-hydration heating, the most obvious effects of which are dehydroxylation of phyllosilicates and concomitant formation of finely

* Corresponding author.
E-mail address: matthieu.clog@glasgow.ac.uk (M. Clog).

https://doi.org/10.1016/j.gca.2024.01.023
Received 30 August 2023; Accepted 23 January 2024
Available online 28 January 2024

crystalline olivine (Nakamura, 2005; Tonui et al., 2014; Lee et al., 2016). The potential driver(s) of this late-stage heating include radiogenic decay, solar irradiation, and impacts (Nakamura, 2005; Tonui et al., 2014; Amsellem et al., 2020, Fujiya et al., 2022).

Many CM meteorites are breccias, and most of the clasts in these fragmental rocks are CM lithologies (termed 'cognate clasts') (Bischoff et al., 2006). Brecciation and mixing took place after aqueous alteration (e.g., Lindgren et al., 2013, Verdier-Paoletti et al., 2019), and many of the clasts are likely to have been redistributed from other parts of the same parent body (Yang et al., 2022). Rare clasts of non-CM lithologies (i.e., xenoliths) also occur in the CMs and were likely sourced from other chondritic parent bodies (Fuchs et al., 1973; Zhang et al., 2010; Lee et al., 2023a,2023b).

CM meteorites can provide valuable insights into processes that took place in the protoplanetary disk including aqueous alteration. The liquid water that was responsible for aqueous alteration of the CM parent body (ies) was most likely derived from the melting of accreted ices in response to the decay of ^{26}Al (Grimm and McSween, 1989), although impact-heating may also have played a role (Rubin, 2012). The degree of aqueous alteration of a CM can be quantified by three schemes that variably use the mineralogy, chemical composition and abundance of primary constituents and/or alteration products: (i) the ratio of phyllosilicates to anhydrous silicates as measured by X-ray diffraction of bulk samples (Howard et al., 2009,2011,2015); (ii) the amount of H per unit of mass of bulk sample, contained in either water or hydroxyls (Alexander et al., 2013, Vacher et al., 2020, Lee et al., 2023a,2023b); and (iii) a combination of petrographic and chemical properties determined by in-situ imaging and microanalysis of polished samples (Rubin et al., 2007,2015). Using these classifications, the CM group can be subdivided by petrologic type (Alexander et al., 2013; Howard et al., 2015) or subtype (Rubin et al., 2007). Meteorites with a petrologic type/subtype of 1.0/CM2.0 have been completely aqueously altered whereas those of a potential petrologic type/subtype of 3.0/CM3.0 would be completely unaltered and anhydrous (Rubin et al., 2007; Howard et al., 2015; King et al., 2017). There is a considerable range in the bulk oxygen isotopic compositions of the CMs, which has been interpreted to reflect variable degrees of isotopic exchange between ^{16}O-poor water and ^{16}O-rich primary anhydrous silicates in a closed system (Clayton and Mayeda, 1984,1999). On average, more highly aqueously altered meteorites tend to have a higher whole-rock Δ^{17}O (Rubin et al., 2007), and also have a lower bulk δD (Alexander et al., 2012,2013; Lee et al., 2021a). However, this is not systematic and there is no direct relationship between where a meteorite plots on a three-isotope diagram (i.e., δ^{17}O vs δ^{18}O) and its petrologic sub(type) This apparent inconsistency between bulk oxygen isotopic composition and the closed system model could be reconciled if water ice and/or anhydrous silicates did not have the same initial isotopic composition in all parent body regions, and/or the system periodically experienced mixing between isotopically distinct fluids from different parts of the parent body.

The nature of aqueous alteration during the thermal evolution of the CMs has been debated extensively, with temperatures ranging from subzero to ~160 °C being determined from a variety of geothermometers including organic matter spectroscopy, calcite O isotopes, tochilinite chemistry, phyllosilicate-carbonate fractionation, and dolomite-magnetite fractionation. These measurements typically provide a single temperature for each meteorite, although all CMs must have undergone at least one heating–cooling cycle (Vacher et al., 2019a). Depending on when during the thermal cycle(s) the relevant geothermometer formed or was modified, the value obtained will represent peak temperature, or one point on the curve (e.g., carbonates and phyllosilicates could have formed during heating and/or cooling, whereas insoluble organic matter will record peak temperature that could even have been attained at any time, including after aqueous alteration).

We aim to better understand the thermal, isotopic and chemical evolution of CM parent body(ies) during early solar system history, and to refine the clumped isotope technique for carbonates in meteorite samples. Therefore, we have used the clumped isotope thermometer to determine the temperatures reached in the CM parent body(ies) during aqueous alteration and the growth of carbonate minerals. The carbonate clumped isotope thermometer relies on measuring the distribution of heavy isotopes. At thermodynamic equilibrium, the relative proportion of different isotopologues are a function of temperature. This thermometer is independent of the isotopic composition of co-existing phases. In addition, we explore: (i) if there is a relationship between temperature of carbonate crystal growth and petrologic (sub)type such that the more highly altered meteorites experienced different temperatures; (ii) whether calcite and dolomite grew at the same or different points during thermal evolution; and (iii) how water composition evolved, and how it varied between meteorites and the precipitation of different carbonate minerals.

2. CM Carbonates

Carbonates are a volumetrically minor product of aqueous alteration of the CMs (less than 5 vol%; Lee et al., 2014; Howard et al., 2015) yet offer the potential to reconstruct the thermal, chemical and isotopic evolution of CM parent body(ies). Calcite is present in all CMs. It may be accompanied by aragonite in the moderately to mildly aqueously altered meteorites (Barber 1980; Lee and Ellen, 2008; Lee et al., 2014; Farsang et al., 2021) and by dolomite in the highly aqueously altered ones (Rubin et al., 2007; de Leuw et al., 2010; Lee et al., 2014). Ankerite and breunnerite have been described from one CM, Queen Alexandra Range (QUE) 93005, where they are intergrown with calcite and dolomite (Lee et al. 2012).

Calcite and dolomite have been dated using the ^{53}Mn-^{53}Cr system to 4563 $+0.4/-0.5$ Ma, which is ~4.8 Ma after formation of Calcium- and AIuminium-rich Inclusions (CAIs) (Fujiya et al., 2012). These dates are consistent with radioisotopic ages of 4 ± 2 Ma after CAI formation determined for carbonates from CM and Ivuna-like (CI) meteorites, and CM and CI clasts in other meteorite groups (Visser et al., 2020). This chronology supports the model of liquid generation primarily by ^{26}Al heating (Fujiya et al., 2012; Visser et al., 2020).

The ^{16}O-poor compositions of aragonite grains and their petrographic relationships with calcite suggest that they were the first carbonate to crystallize and formed in a single episode in any one meteorite (Lee and Ellen, 2008; Lee et al., 2013,2014). Likewise, there is no evidence for more than one generation of dolomite in a given CM. However, three generations of calcite have been recognised from their distinctive petrographic characteristics and oxygen isotopic compositions (Tyra et al., 2012,2016; Lee et al., 2013,2014; Fujiya et al., 2015; Vacher et al., 2017,2018). Tyra et al. (2012) found that grains of Type 1 calcite in the Elephant Moraine (EET) 96006-paired meteorites are small, blocky, and inclusion-free, with relatively high δ^{18}O and Δ^{17}O values. Conversely, Type 2 grains comprise larger aggregates of calcite with abundant sulphide inclusions and lower δ^{18}O and Δ^{17}O. Tyra et al. (2012) used the closed system model of Clayton and Mayeda (1999) to interpret these isotopic differences and concluded that Type 2 calcite post-dated Type 1 calcite, and formed from fluids that were more evolved (richer in ^{16}O) owing to a greater degree of interaction with anhydrous silicates. Typically, Type 2 grains have formed by replacement of anhydrous silicates (Tyra et al., 2012), but ^{16}O-rich Type 2 calcite can also occur as veins (Lee et al., 2013; Vacher et al., 2018). The fluids responsible for Type 2 calcite may have been sourced via impact-formed fractures from elsewhere in the parent body (i.e., an open system) (Lee et al., 2013; Vacher et al., 2018). This classification of calcite has subsequently been expanded to include Type 0 grains, which lack the tochilinite-cronstedtite intergrowth (TCI) rims of Type 1 grains, and postdate Type 1 calcite (Vacher et al., 2017).

3. Samples and methods

3.1. Sample description and characterization

The samples selected for this study have been mildly to highly aqueously altered and so span a range in petrologic (sub)types (Table 1). None have evidence for being heated after aqueous alteration. This study has used both falls (Cold Bokkeveld, Murchison) and Antarctic finds (Allan Hills (ALH) 83100, LaPaz Icefield (LAP) 031166, Lonewolf Nunataks (LON) 94101, Scott Glacier (SCO) 06043). Each meteorite was characterized by Scanning Electron Microscope (SEM) imaging including point counting, and X-ray microanalysis, as described below. The SEM work was undertaken at the University of Glasgow using a Zeiss Sigma SEM equipped with an Oxford Instruments X-Max energy dispersive X-ray (EDX) spectrometer connected to Oxford Instruments INCA and Aztec software. The SEM was operated at 20 kV/3nA and was used for backscattered electron (BSE) imaging, qualitative X-ray microanalysis, and X-ray mapping. All of these meteorites have been characterised by the authors in previous petrographic, chemical and isotopic studies (Lee et al., 2013,2014; Lindgren et al., 2013,2017,2020).

3.1.1. Murchison

Murchison fell in Australia in 1969 (Graham et al., 1985). This study used samples from three different stones that were provided by the Natural History Museum, London (NHM): 1988-M23, 1970-6, and 1970-5, with masses of 1.35, 1.07, and 0.53 g, respectively. Petrography used polished thin sections of all three samples, and chips of the first two were also analysed for their isotopic compositions. Murchison is the least aqueously altered of the CMs studied (Table 1). Its chondrules are set in a fine-grained matrix composed of phyllosilicate and tochilinite-cronstedtite intergrowths. They generally display a porphyritic texture with unaltered ferromagnesian silicates, but the mesostasis and some of the phenocrysts have been altered to phyllosilicate. Fe-Ni metal grains occur in the cores of some chondrules. Murchison contains 1.4 % calcite as determined via point counting, both as single Type 1 grains (Fig. 1a) and some Type 2 replacing chondrules. Aragonite has also been described and is abundant relative to other CMs in which it occurs (3.2 crystals/mm^2; Lee et al., 2014). Dolomite was absent from the studied samples.

Table 1
Details of the samples studied and their petrologic classifications.

CM meteorite	Fall/find, date, initial mass	Petrologic classifications			
		Type[a]	Type[b]	Subtype[c]	Subtype[d]
ALH 83100	Find, 1983, 3019 g	1.1	1.2	CM2.1[g]	——
Cold Bokkeveld	Fall, 1838, 5200 g	1.3	1.4	CM2.2	CM2.1–2.7
LAP 031166	Find, 2003, 15 g	——	——	CM2.1[h]	——
LON 94101	Find, 1994, 2805 g	1.8[e]	1.3 [e]	CM2.2–2.3[h]	CM1–CM3
Murchison	Fall, 1969, >100 kg	1.6	1.5	CM2.5	CM2.7–2.9
SCO 06043	Find, 2006, 28 g	1.1, 1.2[f]	1.2	CM2.0[h]	——

—— denotes not determined.
[a] Scheme of Alexander et al. (2013).
[b] Scheme of Howard et al. (2015).
[c] Scheme of Rubin et al. (2007).
[d] Scheme of Lentfort et al. (2020).
[e] Classification for LON 94102, which may be paired with LON 94101 (Meteoritical Bulletin).
[f] Two samples were classified.
[g] Classified by de Leuw et al. (2010).
[h] Classified by Lee et al. (2014).

3.1.2. LON 94101

This Antarctic find from 1994 has a weathering grade of Be (Grossman and Score, 1996). Its petrologic (sub)type indicates it has been moderately aqueously altered overall, but this meteorite is highly brecciated and contains several clasts that underwent different degrees of aqueous alteration (Lindgren et al., 2013). The clumped isotope work used a 0.49 g chip (LON 94101,67) and petrographic work a polished thin section (LON 94101,15), both provided by ANSMET. The studied sample is consistent with a petrologic subtype of CM2.3 (e.g., chondrules in this meteorite are partially replaced by phyllosilicates and calcite, but some ferromagnesian silicates are preserved). It contains 1.3 % calcite as determined by SEM point counting, which occurs as individual grains in the matrix (Type 1 calcite, Fig. 1b), replacing chondrules (Type 2 calcite), and as a mm-sized calcite vein (Lindgren et al., 2011; Lee et al., 2013). Minor quantities of aragonite also occur; the thin section of LON 94101 studied by Lee et al., (2013,2014) has 0.21 aragonite crystals/mm^2 that are heterogeneously distributed. Dolomite was not observed.

3.1.3. Cold Bokkeveld

Cold Bokkeveld fell in South Africa in 1838 (Graham et al., 1985), and in accordance with its terrestrial age has undergone some alteration during curation (i.e., likely producing gypsum, Lee, 1993; Lee et al., 2021b). This study used samples from three different stones provided by the NHM (CB-13989, 1.35 g; CB-BM1727, 0.98 g; CB-BM1964, 0.44 g). Petrographic work used polished thin sections made from all three, and chips of the first two were used for clumped isotope measurements. Cold Bokkeveld is typically described as a highly aqueously altered CM with a correspondingly low petrologic (sub)type (Table 1), although it contains clasts that have undergone different degrees of aqueous processing (Greenwood et al., 1994; Lentfort et al., 2020). SEM point counting recorded 1.9 % Ca-carbonate, which is likely to mainly comprise calcite, although minor aragonite has been previously described from other samples (0.03 crystals/mm^2; Lee et al., 2014). Ca-carbonate occurs as single grains in the matrix that are commonly rimmed by serpentine and tochilinite (i.e., Type 1 calcite), but has also been described as partially replacing chondrules and CAIs (i.e., Type 2 calcite; Fig. 1c) (Lee, 1993; Greenwood et al., 1994). No dolomite was point counted in the present study although small quantities have been described from other samples of the meteorite (Johnson and Prinz, 1993; Lee et al., 2014; Farsang et al., 2021).

3.1.4. LAP 031166

This Antarctic find has a weathering grade of B (Connolly et al., 2007). The clumped isotope work used a 0.92 g chip (LAP 031166,21), and petrographic work a polished thin section (LAP 031166,15), both provided by ANSMET. LAP 031166 has been highly aqueously altered and was classified as CM2.1 by Lee et al. (2014) (Table 1). Its chondrules have been heavily replaced although many retain some olivine and pyroxene. SEM point counting recorded 0.8 % Ca-carbonate and no dolomite. The Ca-carbonate occurs as single grains in the matrix that have inclusions of Fe-rich serpentine fibres, themselves encrusted by Fe-Ni sulphide crystals (i.e., Type 1; Fig. 1d). Calcite has also replaced chondrules (i.e., Type 2 calcite) (Lee et al., 2014; Lindgren et al., 2017).

3.1.5. SCO 06043

This Antarctic find has a weathering grade of B/Ce (Weisberg et al., 2008). The clumped isotope work used a 1.24 g chip (SCO 06043,27) and petrographic work a polished thin section (SCO 06043,10), both provided by ANSMET. SCO 06043 has been highly aqueously altered (Table 1). Its fine-grained matrix has a strong petrofabric that is defined by flattened chondrule pseudomorphs (made of phyllosilicates, some with rims and inclusions of sulphides; Lindgren et al. 2015). Calcite and dolomite occur as monomineralic grains, and intergrown as bimineralic grains. Dolomite also forms narrow veins (Lee et al., 2014) (Fig. 1e). Point counting shows that the thin section contains 0.6 % calcite and 0.9 % dolomite.

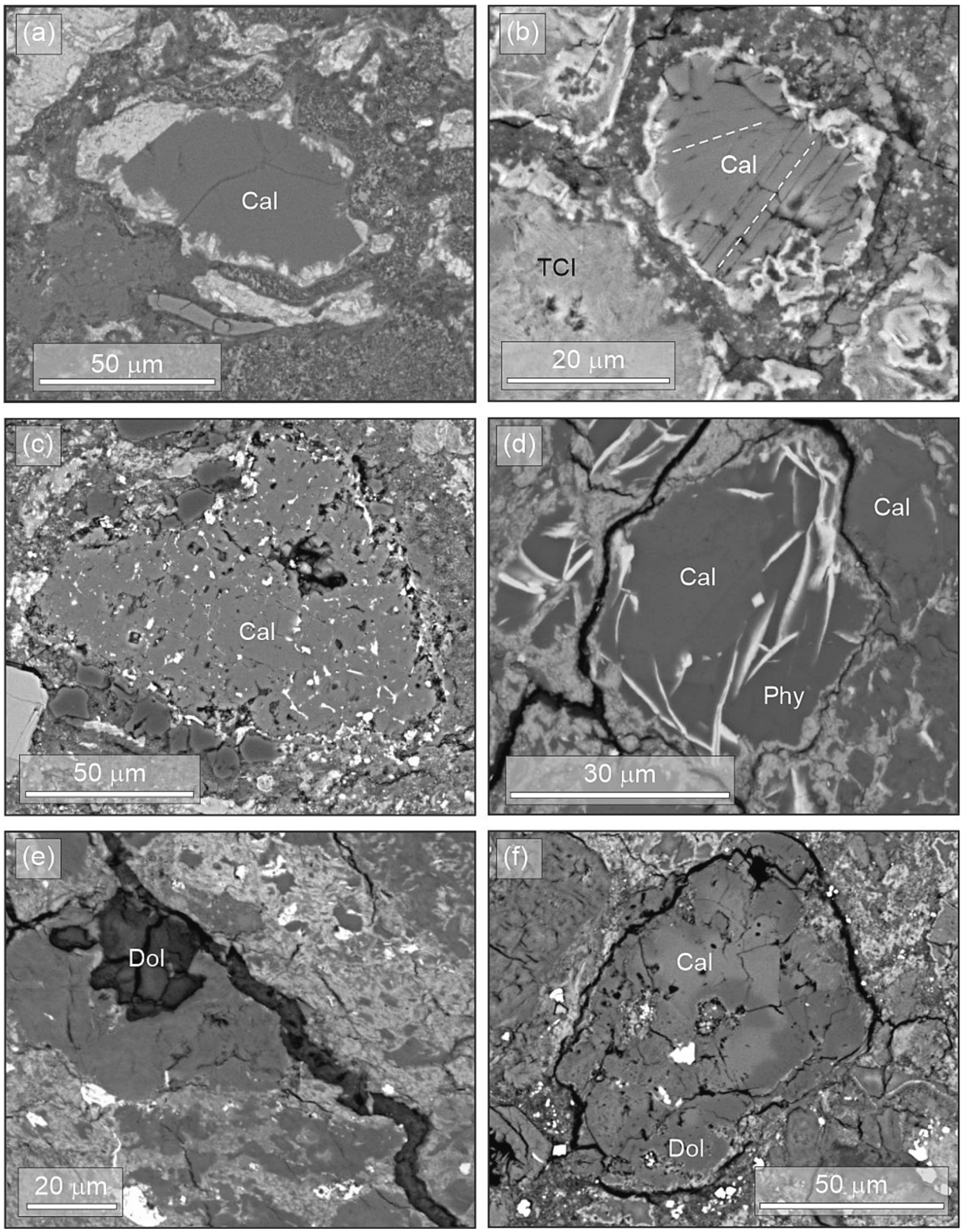

Fig. 1. BSE images of calcite (Cal) and dolomite (Dol) in the studied meteorites. (a) Murchison type 1 calcite grain (centre of image) that is enclosed by TCI and set in a fine-grained phyllosilicate matrix. (b) LON 94101 type 1 calcite grain that is twinned in two orientations as indicated by the dashed white lines. The fine-grained matrix of the host meteorite contains several TCIs. (c) Cold Bokkeveld type 2 calcite grain replacing a chondrule. White specks are sulphide inclusions. (d) LAP 031166 type 1 calcite grain that has been partly replaced by phyllosilicates (Phy). The white needles are fibres of Fe-rich serpentine encrusted by Fe-Ni sulphide. (e) SCO 06043 dolomite grain that is adjacent to a thin vein of dolomite (oriented NW-SE in the image). (f) ALH 83100 bimineralic carbonate grain containing an intergrowth of calcite (light grey) and dolomite (darker grey).

3.1.6. ALH 83100

ALH 83100 is an Antarctic find with a weathering grade of Be (Grossman, 1994). The clumped isotope work used a 1.640 g chip provided by ANSMET (ALH 83100,276), and petrographic work a polished fragment made from the chip. This meteorite has a low petrologic (sub) type indicating a high degree of aqueous alteration (Table 1). It is composed of partially to completely aqueously altered chondrules set in a fine-grained phyllosilicate-rich matrix. The chondrules have been altered to phyllosilicates and sometimes carbonates. The matrix includes grains of anhydrous silicates, sulphides (pyrrhotite, pentlandite and tochilinite; Lindgren et al., 2020), and carbonates (calcite and dolomite, as monomineralic grains and intergrown as bimineralic grains; Lee et al., 2014) (Fig. 1f). SEM point counting recorded 1.2 % calcite and 2.1 % dolomite and so this specimen has the highest proportion of dolomite out of the samples studied.

3.2. Sample stable isotope measurements

Sample preparation and isotopic analyses described below were performed at the Scottish Universities Environmental Centre (SUERC).

3.2.1. Sample preparation

Meteorite chips were rinsed with distilled water, dried, and then crushed with an agate mortar and pestle. The powder was sieved to a grain size of <56 μm to promote quick reaction with the phosphoric acid in the next stage, and to limit the potential for grains of carbonates to be completely enclosed by non-reactive minerals, which would hinder the yield of CO_2.

We also prepared a 'fake meteorite' control sample to test whether having carbonates in a sample as only a minor phase would impact the preparation process and lead to offsets in the measured clumped isotope compositions (see Supplementary Information (SI)). We used a Carrara marble of known bulk and clumped isotopic composition, pyrite and a Jurassic carbonaceous sandstone from Torr Mor in Scotland (Anderson and Dunham, 1966). All three were crushed together in the following proportions by weight: marble 1 %, pyrite 5 %, sandstone 94 %. The aims were to ensure that: (i) the acid digestion and CO_2 purification of the mixture led to a CO_2 yield corresponding to its carbonate fraction, and (ii) the clumped isotope composition measured for the gas extracted control sample was within error of that of the pure carbonate. There is no terrestrial rock that perfectly mimics the matrix of our samples. The Torr Mor sandstone contains detrital silicates, iron oxides and organic matter, which are also present in the matrices of carbonaceous chondrites.

3.2.2. CO_2 extraction and gas purification

Meteorite samples (from 100 to 400 mg) were digested under vacuum in >103 % H_3PO_4 in an acid bath with constant agitation using a magnetic stirrer to promote the dispersion of the powder throughout the acid. Samples containing only calcite, or a negligible amount of dolomite (Cold Bokkeveld) were reacted at 90 °C for 30 min. For samples containing both calcite and dolomite, we proceeded in two steps. First, to extract the calcite portion, an aliquot of sample powder was reacted at 25 °C for 1 h. The shorter duration compared to previous studies (e.g., Benedix et al.,2003 or Guo and Eiler, 2007 who use 24 h digestion) is justified by the smaller grain size of the powder and constant agitation used. Second, another aliquot of powder was reacted at 90 °C for 2 h to completely dissolve both calcite and dolomite. The isotopic composition of the dolomite fraction was calculated using the results of the two steps, described further below. A similar method was employed by Lloyd et al. (2017) to measure clumped isotope compositions of calcite and dolomite coexisting in the same sample.

In all cases, gases produced were trapped in a metal coil submerged in liquid nitrogen and placed immediately next to the acid vessel in the vacuum line. In the last 3 min of acid digestion (5 min for dolomite), non-condensable gases were evacuated using a turbomolecular pump. After the chosen time had elapsed, the acid bath was isolated and the metal trap was submerged with a propanol-dry ice slush (temperature approximately −76 °C), liberating CO_2 and some other gaseous species but not water. The gas was passed over tightly packed silver wool to remove some of the sulfur-bearing gases, then a glass coil cooled with a propanol-dry ice slush. The gas was frozen in a further glass coil submerged in liquid nitrogen. The resulting gases were then transferred to a calibrated volume attached to a strain gauge using liquid N_2. The gas was thawed until it reached room temperature, after which the acid digestion volume yield was measured. The gas was then passed through a 4 m Gas Chromatography (GC) column held at 40 °C with He carrier gas, which removed contaminants such as sulfur-bearing gases and hydrocarbons, before being diverted to a first Ion Ratio Mass Spectrometer for clumped isotope measurement. Consistent with the observation of Guo and Eiler (2007), we found that sulfur contaminants can account for up to 50 % of the total volume of gas. The amount of CO_2 extracted from each sample was similar to amounts obtained from the masses of carbonate standards used for normalization, to avoid the artefacts during GC purification.

3.2.3. Clumped isotope measurements

Clumped isotope measurements were performed with a Thermo Fisher Scientific MAT253 Isotope Ratio Mass Spectrometer (IRMS). Gas was measured in a minimum of 7 blocks of 6 dual-inlet measurements (26 s integration time), recording intensities of m/z 44 to 48. We report the clumped isotope compositions as Δ_{47} defined as:

$$\Delta_{47} = R^{47}/R^{47^*} - 1$$

where R^{47} is the ratio of the abundances of isotopologues with a cardinal mass of 47 (chiefly $^{13}C^{16}O^{18}O$) to the abundance of the isotopologue with mass 44 ($^{12}C^{16}O_2$), and R^{47^*} is the stochastic ratio, calculated using measured $\delta^{13}C$, $\delta^{18}O$, and for our samples, $\Delta^{17}O$.

The intensity of mass 48 was used to screen for contamination of the gas, and we did not systematically achieve complete suppression of contaminants on m/z 48. However, we did not observe any relationship between the intensities on m/z 48 and Δ_{47}, suggesting that there is no isobar on mass 47 from the contaminants. This result is consistent with the contaminants being derived from sulfurous species like SO_2, which can form SO^+ ions that will affect m/z 48 and above, but not 47.

At the end of the clumped isotope measurements, the leftover sample gas was frozen into silica glass tubes using liquid nitrogen. The tubes were flame-sealed and stored until oxygen isotope analysis was performed, as described in the next subsection.

3.2.4. $\Delta^{17}O$ measurements

Carbonates in CM chondrites have a $\Delta^{17}O$ composition different to terrestrial carbonates (Clayton et al., 1984; Benedix et al.,2003; Verdier-Paoletti et al., 2017). While there is subtle variability in terrestrial carbonates (e.g., Passey et al., 2014), the magnitude is not large compared to the analytical uncertainty of clumped isotope thermometry. However, that is not the case for CM chondrite carbonates, where the $\Delta^{17}O$ can differ by more than 1 permil from terrestrial materials. Guo and Eiler (2007) used $\Delta^{17}O$ values from the same meteorites as reported by Benedix et al. (2003), but it is likely that different stones or splits from a single meteorite will differ in $\Delta^{17}O$. Thus, assuming a single $\Delta^{17}O$ value for all samples of a given meteorite is inappropriate and may introduce errors.

Triple isotope oxygen compositions of the CO_2 from the acid digestion of our samples were measured at SUERC with a Thermo Fisher Ultra High-Resolution IRMS using the same gas aliquots as utilized for clumped isotope measurements. The sealed silica tubes were inserted into a tube cracker, and the sample gas expanded into the bellows of the Ultra HR-IRMS. The method of Adnew et al. (2019) was used. Briefly, the oxygen fragments at m/z 16, 17 and 18 created during the ionization of CO_2 are measured. Isobars at these masses (primarily H_2O and OH) are

cleanly resolved due to the high mass resolving power of the instrument (text and Fig. S1 in SI).

The gas used as a working standard was obtained by acid digestion of a calcite with a known $\delta^{18}O$, which is close to that of our meteorite samples. The gas was purified using the same extraction line and GC as the meteorite samples. The uncertainties on the $\delta^{17}O$ and $\delta^{18}O$ decreased with the total numbers of counts registered and the main limit on the precision was counting statistics. Typical precision reached for $\Delta^{17}O$ was lower than 0.1 ‰ (1 standard error) for a single aliquot of CO_2. The CO_2 derived from the digestion of carbonate standards ETH1 to ETH4 was analyzed and found to have a $\Delta^{17}O$ within error of 0, as expected (detailed in SI).

3.2.5. Data processing and normalization

Data reduction was performed using the Easotope software (John and Bowen, 2016) and Python scripts for the $\Delta^{17}O$ corrections and dolomite calculations. We used the IUPAC parameters, in particular $\lambda = 0.528$ (Brandt et al., 2010, Petersen et al., 2019), and the ^{18}O acid fractionations of Kim et al. (2007) and Rosenbaum and Sheppard (1986) for calcite and dolomite, respectively. To define the empirical transfer function (ETF) from the measured Δ_{47} to the absolute reference frames for the different analytical sessions, we used the values from Bernasconi et al. (2021) for the ETH1 to ETH4 carbonate standards. To adjust the Δ_{47} from calcites reacted at 25 °C to 90 °C we used the acid fractionation factor from Petersen et al. (2019). The reprojected Δ_{47} values were used to calculate apparent temperatures using the calibration of Anderson et al. (2021).

$$\Delta_{47\ CDES90} = 0.0391(\pm 0.0004)*10^6/T^2 + 0.154(\pm 0.004)$$

Analytical uncertainties on Δ_{47} were calculated by taking the larger of the standard deviation of the ETH carbonate standard Δ_{47} produced during the measurement period and the standard deviation of replicate measurements of each sample and dividing by the square root of the number of replicates. These calculations also account for the uncertainty due to the difference in bulk isotopic composition between the meteorites and the ETH carbonate standards, following the method presented in Daëron (2021) and using the code attached to that paper (see SI). This uncertainty is particularly important to take into account in our study because we chose a carbonate-based standardization, and the ETH standards have bulk isotope compositions that do not bracket those of CM chondrites. We chose to avoid using CO_2 equilibrated at different temperatures for our standardization to: 1) treat standards and samples the same, and 2) to avoid potential issues with partial re-equilibration of CO_2 to a different clumped isotope composition (i.e., Bernasconi et al., 2021).

Our study is the first to report both the clumped isotope and triple oxygen isotope compositions of carbonate in meteorites as measured from the same sample material. Using CO_2 extracted from each sample replicate for both mass 47 isotopologues and $\Delta^{17}O$ measurements avoids complications or offsets derived from different sample digestion or purification methods. Moreover, the extractions at different temperatures allowed us to differentiate between calcite and dolomite, which has previously been employed for $\Delta^{17}O$ measurements (e.g., Benedix et al., 2003), but not for determination of clumped isotope compositions. This approach avoids making the assumption of homogeneous $\Delta^{17}O$ compositions of each meteorite for correction of clumped isotope data (e.g., Guo and Eiler, 2007).

4. Results

4.1. Carbon and oxygen isotope compositions

Data are presented in Table 2 and Fig. 2. The $\delta^{13}C$ of the carbonates in our samples ranges from +35 to +55 ‰ vs PDB, and $\delta^{18}O$ from +16 to +32 ‰ vs SMOW. We analyzed two different splits of Murchison and Cold Bokkeveld, and for both there was a significant difference between them (up to 4 ‰difference in $\delta^{13}C$ for the Cold Bokkeveld splits). For Murchison, we do not observe the elevated (>60 ‰ vs PDB) $\delta^{13}C$ values that Guo and Eiler (2007) reported. The overall distribution of bulk carbonate isotope compositions is consistent with analyses of bulk carbonates in CM samples reported by Alexander et al. (2015) (Fig. 2). Specifically, carbonates in the more highly aqueously altered meteorites have a lower $\delta^{18}O$ and $\delta^{13}C$ (i.e., enrichment in the heavy rare isotope is reduced proportionally with increased alteration).

The $\Delta^{17}O$ of our samples ranges from −2.57 to −0.96 ‰, with those that are more aqueously altered having a lower $\Delta^{17}O$ (Fig. 3). This result is broadly in agreement with the trend observed for bulk CM carbonates by Benedix et al. (2003). Where calcite and dolomite occur in the same sample, dolomite has a lower $\Delta^{17}O$. Contrary to the study of Benedix et al. (2003), we did not record any dolomite in the samples of Murchison and Cold Bokkeveld that we analyzed (section 2.1). Benedix et al. (2003) observed no differences in the $\Delta^{17}O$ of co-existing calcites and dolomites in the meteorites they analyzed, but none of their samples were more highly aqueously altered than Cold Bokkeveld. In our sample series, however, dolomite is observed and was analyzed in two samples that are more aqueously altered than Cold Bokkeveld (SCO 06043 and ALH 83100).

The two splits of Murchison have $\Delta^{17}O$ within analytical uncertainty of each other, while the two from Cold Bokkeveld display a small but significant difference. The ranges observed for Murchison and Cold Bokkeveld are also consistent with the data from Benedix et al. (2003) (although they analyzed different sample splits) as well as with in-situ carbonate data from Lindgren et al. (2017). However, other in-situ studies have reported positive $\Delta^{17}O$ for the meteorites studied here, as summarized in Table 3.

Table 2
Results of the isotopic measurements on our sample suite and temperatures derived from clumped isotope measurements. Samples measured in two different analytical sessions appear as separate entries. The number of replicates for Dolomite is noted NaN as they are the results of a calculation from separate analyses of the calcite only and the sum of all carbonates (see Methods section and SI).

Meteorite	Split	Min.	n	$\delta^{13}C$ (‰)	± (‰)	$\delta^{18}O$ (‰)	± (‰)	$\Delta^{17}O$ (‰)	± (‰)	Δ_{47}c (‰)	± (‰)	T (°C)	± (°C)
ALH 83100	,276	C	3	36.20	0.48	25.61	0.18	−1.96	0.05	0.526	0.018	51.2	7.9
ALH 83100	,276	D	NaN	50.01	0.20	19.79	0.20	−2.57	0.12	0.433	0.024	101.4	16.2
Cold Bokk	CB13989	C	4	46.64	0.21	30.02	0.13	−1.47	0.07	0.589	0.023	26.8	7.9
Cold Bokk	CB13989	C	1	46.65	0.20	30.53	0.20	−1.56	0.07	0.591	0.021	26.1	7.2
Cold Bokk	BM1727	C	4	50.62	0.25	27.11	0.14	−1.86	0.08	0.567	0.018	34.7	6.7
LAP 031,166	,21	C	4	37.92	0.38	20.47	0.24	−1.91	0.07	0.539	0.027	45.7	11.2
LON 94,101	,67	C	3	55.34	0.07	29.35	0.09	−1.55	0.05	0.631	0.019	13.3	5.7
Murchison	1970–06	C	5	41.59	0.17	31.93	0.16	−0.96	0.05	0.603	0.017	22.1	5.6
Murchison	1988-M23	C	1	42.92	0.20	28.35	0.20	−1.1	0.15	0.66	0.025	5.0	6.9
Murchison	1988-M23	C	2	44.86	0.48	29.69	0.28	−1.07	0.05	0.616	0.029	17.9	9.2
SCO 06,043	,27	C	1	37.20	0.20	22.45	0.20	−1.88	0.06	0.554	0.021	39.6	8.2
SCO 06,043	,27	D	NaN	42.05	0.20	16.18	0.20	−2.46	0.12	0.476	0.028	75.5	15.2

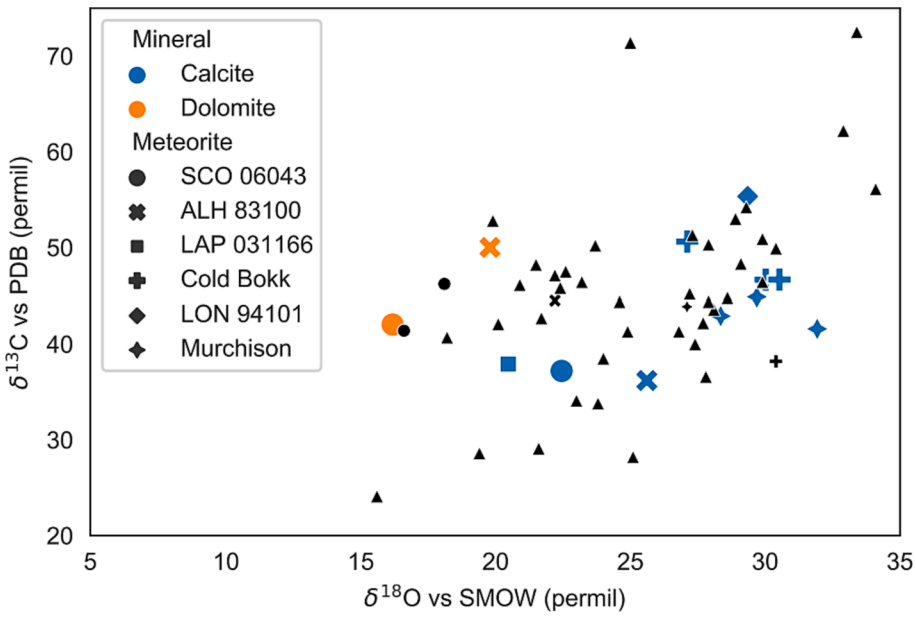

Fig. 2. Bulk isotopic compositions measured on our sample suite. Symbol shapes correspond to the different meteorites and color to the minerals, and are kept for all subsequent figures. Small black symbols are from Alexander et al (2015) where all carbonates were pooled, triangles are meteorites that were not in our sample suite.

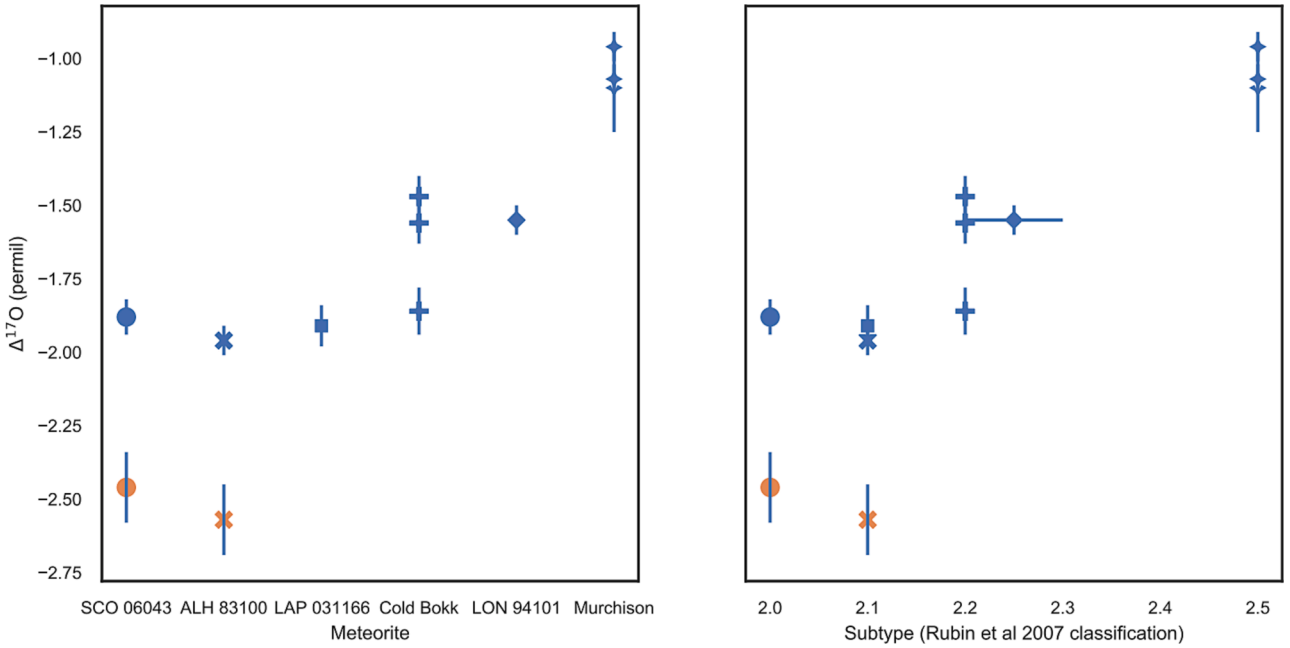

Fig. 3. Δ^{17}O measured on our sample suite. Samples are sorted by petrologic type, from the most altered to the least (left panel) and according to the petrographic subtype (Rubin et al., 2007 classification, right panel).

4.2. Clumped isotope thermometry

After taking into account the differences in Δ^{17}O of carbonates in the samples, the temperatures of carbonate formation calculated from their clumped isotope compositions range from 5 to 51 °C for calcite, and from 75 to 101 °C for dolomite, as illustrated in Fig. 4. In Table 2, we report as individual results, measurements performed in different analytical sessions (for two Murchison and two Cold Bokkeveld splits) as well as two groups of measurements for ALH 83100. These measurements show good agreement. The general trend observed is increasing temperatures of carbonate crystal growth with increasing degree of aqueous alteration of the host meteorite (Fig. 4). Where the two carbonate minerals co-exist (SCO 06,043 and ALH 83100), dolomite records higher formation temperatures (by 35 to 50 °C) than calcite. Guo and Eiler (2007) had previously measured clumped isotope compositions on three chondrites, including Murchison and Cold Bokkeveld. Despite using the bulk Δ^{17}O from Benedix et al. (2003), their reported temperatures of 20–33 °C for Murchison and 26–71 °C for Cold Bokkeveld are consistent with our results, although our range of temperatures for Cold Bokkeveld is significantly narrower (26–35 °C).

Table 3
Comparison of average $\Delta^{17}O$ measured on meteorites in our sample set by bulk (this study, Benedix et al., 2003) and in situ techniques (all others).

$\Delta^{17}O$	Our data	Benedix et al. (2003)	Lee et al. (2013)	Fujiya et al. (2015)	Lindgren et al. (2017)	Verdier Paoletti et al. (2017)	Telus et al. (2019)
Murchison	−1.05 ± 0.10	−0.82 ± 0.05		0.7 ± 0.9	−1.6 ± 1.7	1.3 ± 0.9	
Cold B	−1.64 ± 0.10	−1.65 ± 0.05			−1.7 ± 1.8	0.3 ± 0.9	
LON 94,101	−1.54 ± 0.08		1.4 ± 1.1				
LAP 031166	−1.91 ± 0.10				0 ± 1.8		
ALH 83100 calcite	−1.96 ± 0.10						0.5 ± 2
ALH 83100 dolomite	−2.57 ± 0.12						0.8 ± 2

± is the standard deviation of multiple measurements.

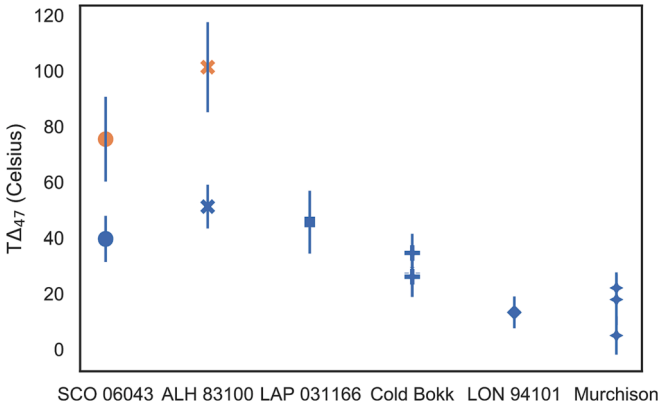

Fig. 4. Temperatures derived from the measured Δ_{47}, after taking into account the $\Delta^{17}O$.

5. Discussion

5.1. Significance of the temperatures derived from clumped isotope measurements

Many CM carbonaceous chondrites are breccias whose constituent clasts can contain carbonates that formed in different environments and/or at different times (i.e., within contrasting parts of the same parent body or even in different bodies). Thus, none of the samples analyzed here are likely to contain a single carbonate generation. This heterogeneity in carbonate populations is demonstrated by petrographic results (Section 2) showing the co-existence of several generations of Ca-carbonate in some meteorites (e.g., Types 1 and 2 calcite), and intergrowths of calcite with dolomite.

Despite this heterogeneity, the range in oxygen isotopic composition of Ca-carbonate as measured by ion microprobe is similar between meteorites. For example, in the EET 96006-paired meteorites Tyra et al. (2012) recorded ranges for $\delta^{18}O$, $\delta^{17}O$ and $\Delta^{17}O$ of 21.0, 14.8 and 5.5 ‰, respectively. With regards to $\delta^{13}C$, the ranges can be considerably greater. Fujiya et al. (2019) recorded a maximum 50.7 ‰ difference between analyses of LAP 31166 Ca-carbonate, and 35.1 ‰ for Nogoya. Similarly, Vacher et al. (2018) found a range of 46 ‰ for Boriskino, although Fujiya et al. (2020) described a narrower range of 15 ‰ for Yamato (Y) 791198. Distinct Ca-carbonate generations cluster around different values (e.g., Tyra et al., 2012; Fujiya et al., 2015). In-situ analyses of dolomite oxygen isotopic compositions have a considerably narrower range. For Sutter's Mill Jenniskens et al. (2012) reported differences of 2.6, 1.8 and 1.2 ‰ between minimum and maximum values of $\delta^{18}O$, $\delta^{17}O$ and $\Delta^{17}O$, respectively, and Tyra et al. (2016) reported ranges of 6.9, 5.6 and 4.0 ‰ for ALH 84049. The compositional range of carbonates in any one meteorite are a potential source of concern for the interpretation of temperatures derived from clumped isotope measurements, as our bulk data will average intra- and inter-grain variations in carbon and oxygen isotopic compositions. Therefore, the values calculated here represent the averaged composition of the carbonates that are dissolved by the acid. It is a source of bias for the temperature calculated from measured Δ_{47}, as mixing is non-linear for Δ_{47} (Eiler and Schauble, 2004, Defliese and Lohmann, 2015).

We have evaluated the magnitude of potential bias using a scenario relevant to our meteorites. Carbonate oxygen isotope data from Lee et al., (2013, excluding data from a calcite vein), Fujiya et al. (2015), Lindgren et al. (2017), Verdier-Paoletti et al. (2017) and Telus et al. (2019) generally show, for meteorites in our sample set, ranges of $\delta^{18}O$ values for Type 1 and Type 2 calcites which can overlap rather two endmembers with distinct, tightly clustered isotopic compositions. Relevant in-situ carbon isotope data are more limited. Fujiya et al. (2015) reported two populations of calcite grains in Murchison with a difference in $\delta^{13}C$ of 40 ‰ (and no difference in $\delta^{18}O$), although one of the populations was only present in a small part of their thin section and represented only a minor portion of the Ca-carbonate grains. Telus et al. (2019) report a range of less than 20 ‰ for $\delta^{13}C$ of calcite in ALH 83100.

We have therefore calculated the offset that would be caused by the mixing of a population of carbonates with a total range of 15 ‰ in both $\delta^{13}C$ and $\delta^{18}O$ values. We chose to have 10 different compositions evenly distributed from one endmember to the other, all present in equal amounts. It is worth noting that this is a worst-case scenario, and that the offset caused by having a non-homogeneous distribution would be lower. We found that the mixing created positive offsets in Δ_{47} of about 0.020 ‰, which is similar to the standard deviation observed on carbonate standards and hence accounted for by our reported uncertainties in temperature.

The interpretation of the calculated temperatures should be considered carefully: there are carbonate grains with different isotopic compositions and potentially different formation temperatures in each of our samples. Our reported isotopic values reflect the weighted average (for each sample) of the calcite (or dolomite) present. Likewise, the temperatures calculated reflect a weighted average of the actual mineralization temperature for the carbonate grains present in our meteorites. These grains can have formed at different times and/or temperatures; or come from different areas within the parent body. The temperatures of formation for calcite (or dolomite) are thus indicative of the average conditions of formation of that specific carbonate mineral for each meteorite sample, and the temperature range in our sample set reflects differences in the average conditions of carbonate mineral formation between meteorites.

5.2. Comparison with previous estimates of alteration temperatures from carbonate oxygen isotopes

The clumped isotope study by Guo and Eiler (2007) used triple isotope compositions from Benedix et al. (2003), and a different λ for the calculation of $\Delta^{17}O$ from Benedix et al. (2003) and from our study. Additionally, there have been important developments in the technique and practice of carbonate clumped isotope measurements since that pioneer study (i.e., Petersen et al., 2019 and references therein). Nevertheless, temperatures obtained from our Murchison and Cold Bokkeveld data (~5–22 °C and ~26–35 °C, respectively) are roughly consistent with results from the same two meteorites in Guo and Eiler (2007) (~20–33 °C and ~26–71 °C, respectively). A range of other indirect methods have been used to determine the temperatures reached in CM carbonaceous chondrites (Table 4), and below we evaluate the subset of those that utilized oxygen isotopes.

Alexander et al. (2015) conducted a systematic analysis of carbonate $\delta^{13}C$ and $\delta^{18}O$ values in CM chondrites (black symbols in Fig. 2). They proposed a model where a single fluid would form carbonates at temperatures of 0–130 °C, with higher $\delta^{13}C$ and $\delta^{18}O$ corresponding to lower temperatures of formation. Although this range is at first glance consistent with our observations, Alexander et al. (2015) suggest, based on CO/CO_2 $\delta^{13}C$ values and assuming isotopic equilibrium, that Murchison carbonates would have formed at ~87 °C, while we report 5–22 °C for the same meteorite. Fujiya (2018), using whole-rock $\delta^{18}O$ and δD from a range of CMs, put constraints on the isotopic composition of primordial water, and concluded that carbonate formation occurred below 150 °C.

Verdier-Paoletti et al. (2017) measured $\delta^{17}O$ and $\delta^{18}O$ of carbonates in nine CMs in situ by ion probe and observed that both carbonates and alteration water had variations along lines in ($\delta^{18}O$, $\delta^{17}O$) space, with data defining the same slopes but different intercept values. They assumed that a given carbonate was precipitated from a water defined by the data trend they identified and calculated carbonate formation temperatures of ~110 ± 50 °C in six CM chondrites. They analyzed only two meteorites in common with the present study (Murchison and Cold Bokkeveld) and obtained median temperature estimates of ~160 °C. Vacher et al., (2019b) also used in situ measurements of oxygen isotopic composition of carbonates in CM chondrites along with previous estimates of the compositions of the alteration fluids. Their approach was to calculate the temperature from the apparent isotopic fractionation factor between the carbonates and the fluid. The only sample common to our studies is the Murchison meteorite, where they obtained from 19 ± 22 to 50 ± 34 °C.

If two coexisting mineral phases formed at the same time and at isotopic equilibrium with each other the temperature of carbonate formation can be estimated. Using Murchison, Clayton and Mayeda (1984) first compared $\delta^{18}O$ in calcite and phyllosilicate and concluded that the temperature of formation was below 20 °C. However, as those two phases do not have the same $\Delta^{17}O$ and were therefore not at isotopic equilibrium, temperatures cannot be calculated from the calcite-phyllosilicate fractionation factor. Benedix et al. (2003) proposed that calcite and phyllosilicates in Nogoya (CM2) were at isotopic equilibrium and estimated a temperature of 0–25 °C. From measurements of the oxygen isotopic composition of dolomite and magnetite in ALH 83100, Telus et al. (2019) considered that they were in isotopic equilibrium, and using the dolomite-magnetite $\delta^{18}O$ fractionation they calculated that the dolomite had formed at 120 ± 60 °C. This temperature is similar to the values measured in our study for dolomite in the same meteorite (101 ± 16 °C, Table 2 and Fig. 3), although the analytical uncertainties are large in both techniques.

Table 4
Previously determined temperatures of CM aqueous alteration in chronological order of publication.

Study	Technique	Material analysed	Meteorite	Temperature
Telus et al. (2019)	Magnetite-dolomite oxygen isotope fractionation	Dolomite	ALH 83100	125 ± 60 °C
Vacher et al., (2019a)	Mg content of the hydroxide layer of tochilinite	Tochilinite	Paris	122 ± 38 °C
			Murchison	132 ± 43 °C
			Murray	130 ± 50 °C
			Nogoya	153 ± 47 °C
			Cold Bokkeveld	157 ± 48 °C
Vacher et al., (2019b)	Geochemical modelling	Ca-carbonate	Maribo	−9 ± 11 to 5 ± 14 °C
			Murchison	19 ± 22 to 50 ± 34 °C
			Jbilet Winselwan T1 calcite	15 ± 21 to 33 ± 29 °C
			Jbilet Winselwan T2 calcite	109 ± 11 to 158 ± 22 °C
			Mukundpura T1 calcite	12 ± 17 to 34 ± 22 °C
			Mukundpura T2 calcite	110 ± 32 to 139 ± 55 °C
Verdier-Paoletti et al. (2019)	Geochemical modelling of Verdier-Paoletti et al. (2017)	Ca-carbonate	Boriskino	−13.9 ± 22.4 to 164.2 ± 18.6 °C (average 60.3 ± 74.0 °C)
		Dolomite	Boriskino	32.8 ± 16.1 to 166.5 ± 47.3 °C
Fujiya (2018)	Geochemical modelling	Carbonates	Suite of CMs	<150 °C
Visser et al. (2018)	Raman spectroscopy of organic matter	Organic matter	Murchison	64 ± 25 °C
			Banten	64 ± 25 °C
			Murray	72 ± 19 °C
Verdier-Paoletti et al. (2017)	Geochemical modelling	Ca-carbonates	Nine CMs	113 ± 54 °C
Alexander et al. (2015)	Modelling using empirical bulk calcite oxygen isotope data	Calcite	64 CMs	0–130 °C
Guo and Eiler (2007)	Clumped isotope thermometry	Calcite	Murchison	20–33 °C
			Murray	30 °C
			Cold Bokkeveld	26–71 °C
Busemann et al. (2007)	Raman spectroscopy of organic matter	Organic matter	8 CMs	<220–240 °C
Nakamura et al. (2003)	Dolomite-phyllosilicate oxygen isotope fractionation	Dolomite and matrix	Sayama	>120 °C
Clayton and Mayeda (1999)	Modelling using empirical bulk oxygen isotope data	Bulk meteorites	34 CMs	Near 0 °C
Zolensky et al. (1993)	Stability of serpentine and tochinilite	Serpentine and tochinilite	23 CMs	<50 °C
Clayton et al. (1984)	Calcite-phyllosilicate oxygen isotope fractionation	Calcite and phyllosilicate	Murchison	20 °C or less

(continued on next page)

Table 4 (*continued*)

Study	Technique	Material analysed	Meteorite	Temperature
Bunch and Chang (1980)	Petrographic observations	Matrix minerals	Murchison, Murray, Nogoya	<127 °C
DuFresne and Anders (1962)	X-ray diffraction	Unspecified	Cold Bokkeveld, Mighei, Murray, Haipura	Close to room temperature

5.3. Triple oxygen isotope data and fluid evolution, and relationship with temperature variations

5.3.1. Oxygen isotopic evolution of the fluid-rock system

In ($\delta^{18}O$, $\delta^{17}O$) space (Fig. 5), our carbonate data define a trend with a slope (0.61) which is steeper than the Terrestrial Fractionation Line (TFL, 0.52). Thus, our data cannot be explained by precipitation of carbonates from a single aqueous fluid where only the temperature varied between meteorites; such a process would produce a slope parallel to the TFL. Our slope is consistent with mixing of oxygen from silicates into the aqueous fluids and agrees with the classic closed system model of Clayton and Mayeda (1984, 1999): water evolves toward lower $\Delta^{17}O$ as a result of a greater extent of reaction with the host rock. Our more altered meteorites (according to their petrographic (sub)type, see Table 1 and Fig. 3) contain carbonates that have lower $\Delta^{17}O$ on average, suggesting a common cause for alteration of the silicate matrix and variations in the isotopic composition of carbonates. This slope is also within error of those calculated in previous in situ studies (Tyra et al., 2012, Lee et al., 2013; Vacher et al., 2018; and Verdier-Paoletti et al., 2017; the latter once the Paris meteorite carbonates are removed), but comparison with in-situ data for specific chondrites is less conclusive. As shown in Table 3, our data for Murchison and Cold Bokkeveld are in good agreement with Lindgren et al. (2017), but different from other in situ studies which report values ~2 ‰ higher than our results. The typical analytical uncertainty is greater than ± 1 ‰ for in situ data, versus ± 0.1 ‰ for our method.

5.3.2. Oxygen isotopic composition of water, comparison with carbonate $\delta^{13}C$

We calculate the isotopic composition of the fluids in equilibrium with the carbonates using their temperatures from the clumped isotope measurements. In common with the calculated temperatures, the isotopic compositions determined for the fluid correspond to the mode of a range of fluids that deposited carbonates in a given meteorite. The results are in Table S1 **of the SI**, and in Fig. 6 they are plotted against carbonate $\delta^{13}C$. The $\delta^{18}O$ of the fluid ranges from −6.6 to +2.3 ‰ vs SMOW, which is lower than the values calculated by Guo and Eiler (2007) of 2–8 ‰ or 5 ‰ in the model of Alexander et al. (2015).

We do not observe a trend between $\delta^{13}C$ of the carbonates and $\delta^{18}O$ of the fluid (Fig. 6) in contrast to Guo and Eiler (2007), who suggested that methane was generated alongside carbonate precipitation. However, this conclusion may stem from the very high $\delta^{13}C$ they reported for Murchison (>60 ‰ vs PDB), whereas we found values ranging from 41 to 44 ‰ vs PDB, comparable to the results of Grady et al. (1988) and Alexander et al. (2015). There are no unequivocal trends between $\delta^{18}O$ of the aqueous fluid and the degree of alteration or temperature. This finding argues against a single initial aqueous fluid which, before exchange with silicates, would have been common to all our samples. Fig. 7 compares the estimated oxygen isotopic composition of primary water that was accreted to the CM parent body(ies) with the composition of the carbonate's parent water as calculated in the present study. These data are also listed in **Table S1 of the SI** along with several other estimates of primary water $\Delta^{17}O$ or $\delta^{18}O$. The consensus of previous work is that primary water had a positive $\Delta^{17}O$, whereas the $\Delta^{17}O$ of carbonate parent water determined here is below the TFL. All of the estimates indicate that there was extensive reaction of the primary water with anhydrous silicates prior to carbonate precipitation. The best fit line through the 16 determinations of carbonate parent water has a slope of 0.57 ± 0.04. Although it is close to the slope of the TFL it is important to recognise the relatively large errors in the calculated water compositions due to the relative uncertainties on the temperatures derived from the clumped isotope measurements.

5.4. Increase in carbonate formation temperature with extent of alteration

Our data show a clear correlation between $\Delta^{17}O$ and temperature (Fig. 8), forming a single trend for both calcite and dolomite. We also find that the more aqueously altered meteorites have higher temperatures of carbonate crystallization (Fig. 4). The most parsimonious explanation for these correlations is that the overall extent of aqueous alteration and the average temperature for carbonate precipitation reflect the same process: the overall degree of aqueous alteration increases with temperature. The evolution of $\Delta^{17}O$ of the aqueous fluid towards lower values due to exchange of oxygen atoms with the silicate matrix is also consistent with this interpretation. Our observations are, however, inconsistent with a greater extent of alteration being due to higher water–rock ratios at a common temperature (e.g., calcites in CM chondrites record a range of temperatures of 5-51 °C). We also find that dolomites formed at higher temperatures than calcites when both

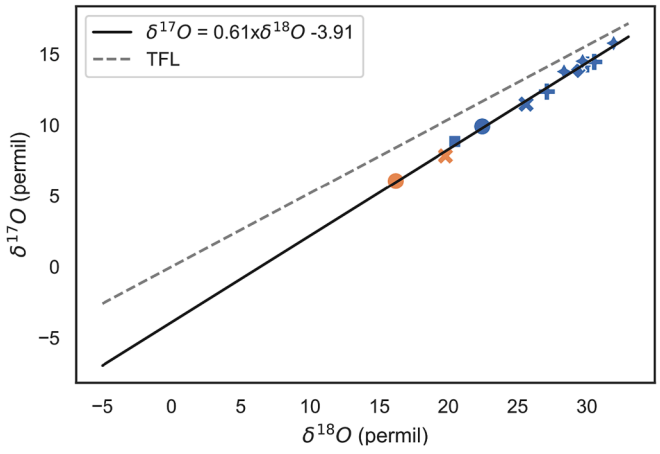

Fig. 5. Oxygen isotope compositions measured in the carbonates. The Terrestrial Fractionation Line and the linear fit to the oxygen isotope data are also displayed.

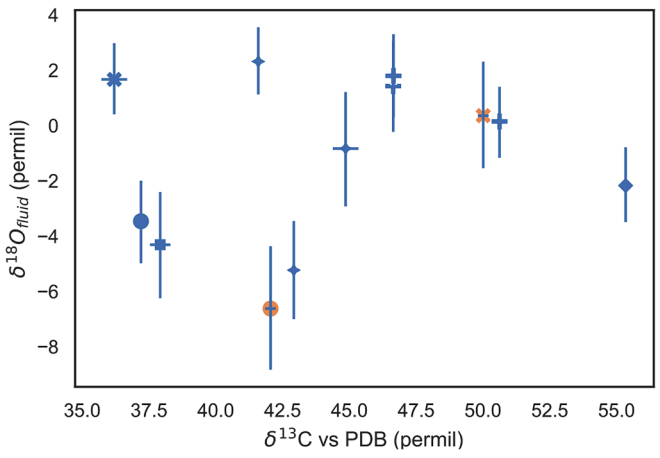

Fig. 6. $\delta^{18}O$ of the fluids against the $\delta^{13}C$ of the carbonate minerals. No relationship is observed.

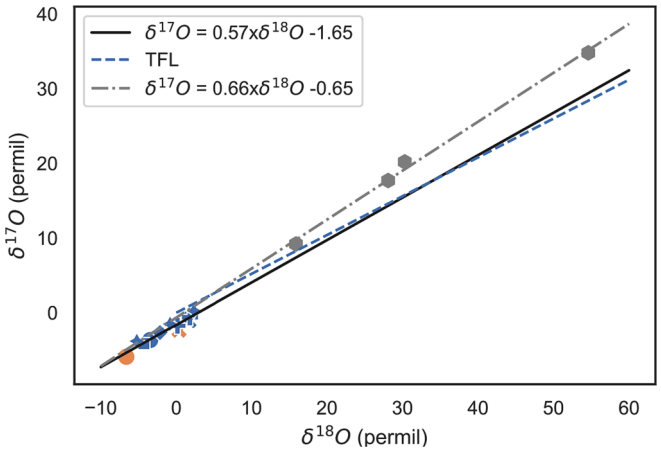

Fig. 7. Oxygen isotope compositions of the fluids in equilibrium with the carbonates (same legend as in the previous plots), compared to prior estimates of the oxygen isotope composition of primary water (in grey, from Clayton and Mayeda (1984), Clayton and Mayeda (1999) and Fujiya (2018)) and to the Terrestrial Fractionation Line.

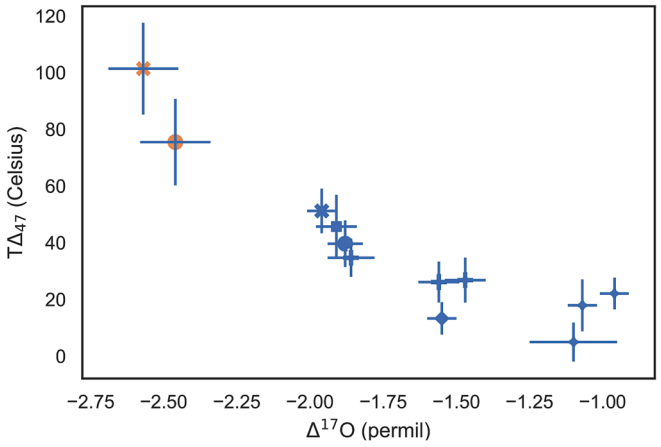

Fig. 8. Temperatures calculated from clumped isotope measurements versus $\Delta^{17}O$.

minerals are present, and from a fluid with a lower $\Delta^{17}O$. These differences suggest that dolomites formed after calcites as the fluids continue to evolve isotopically. Because of the brecciated nature of the CM chondrites, these differences do not however imply that the calcites and dolomites present in the same meteorite sample necessarily formed in the same location on the parent body.

It should be noted that these observations do not exclude the possibility that alteration of the silicate matrix continued after carbonate formation. However, the good correspondence between the temperature of carbonate formation and petrographic (sub)type of the host meteorite (Fig. 4) indicates that further chemical alteration of the matrices was limited in extent and puts constraints on the thermal history after formation of the carbonates.

Clumped isotope signatures recorded in carbonates can be modified by bond reordering when temperatures rise above a given threshold which depends on the carbonate phase, with dolomite clumped isotope signatures being more robust than calcite's (e.g., Stolper and Eiler, 2015, Hemingway and Henkes, 2021). The extent of re-ordering depends on the peak temperature and time spent at high temperature. Conservation of a range of values for the calcites in our sample suite precludes substantial bond reordering. Heat production in the parent bodies mainly comes from the radioactive decay of ^{26}Al (Visser et al., 2020), which is extinct after 5 Ma. Although there is still some uncertainty on the celerity of bond reordering, with competing models of the exact physical process, it would require temperatures of 200 °C or more to completely reorder calcite in a few Ma (Hemingway and Henkes, 2021). A briefer heating event lasting for 1000 years would need to reach temperatures of more than 300 °C to completely overprint initial clumped isotope signatures.

Verdier-Paoletti et al. (2017) calculated carbonate formation temperatures for individual meteorites from their in-situ data and their model is briefly described in subsection 5.2. Although they found variations in $\Delta^{17}O$ with petrographic type that are consistent with our results (Fig. 8 of their paper), they argue that higher $\Delta^{17}O$ was associated with higher T, which is the opposite of our results. Consequently, their interpretation is that calcites are formed before serpentine, at high hydrothermal temperatures (above 100 °C), and that the mineral assemblages reflect a cooling trend from the least altered CM chondrites (Paris and Murchison) to the more altered (e.g., Nogoya in their study). This conclusion requires that the least altered CM chondrites have experienced aqueous fluid circulation at the highest temperatures, which is inconsistent with the results of our study.

5.5. Constraints on parent body evolution from carbonates

5.5.1. Model for carbonate crystal growth

Here we describe a model to account for the correlations between carbonate mineralogy, $\Delta^{17}O$ and temperature, and the host meteorite's degree of aqueous alteration (Fig. 9). The model assumes an initially closed system, that alteration takes place in the interior of a parent body rather than in its regolith, and that is a prograde reaction (i.e., the fluid evolves isotopically as it gets hotter).

The CM parent body(ies) accreted crystalline and amorphous silicates (potentially hydrated, Le Guillou et al., 2019), metal, sulphides, organic matter and ices. Subsequent aequeous alteration was initiated by melting of water ice in response to internal heating, primarily from the decay of ^{26}Al (Grimm and McSween, 1989). Further heat was generated after aqueous alteration started as it is an exothermic

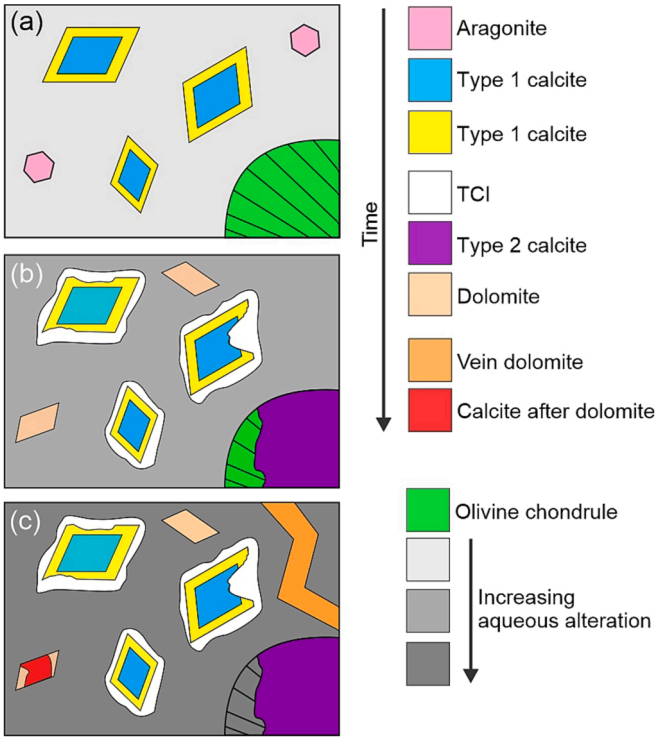

Fig. 9. Cartoon diagrams showing snapshots of a CM lithology during progressive aqueous alteration and carbonate crystal growth.

reaction. Aragonite and type 1 calcite crystallized initially from solutions whose carbon was sourced mainly from volatiles in accreted ices (CO, CO_2, CH_4). Organic matter (especially soluble) and C-rich presolar grains are also potential sources (Alexander et al., 2015; Fujiya et al., 2015; Vacher et al., 2017; Telus et al., 2019), although relative contributions are difficult to ascertain because of the variability in the isotopic composition of the sources and the potential for isotopic fractionation. Sources of calcium will have included CAI-hosted gehlenite (~40 wt% CaO: Lee et al., 2016) and chondrule mesostasis glass (~8–11 wt% CaO; Lee et al., 2016). Fujiya et al. (2020) showed that fluid properties must have changed significantly during growth of the type 1 calcite because crystals in the mildly altered CM Y 791198 are zoned in cathodoluminescence (CL), trace element composition, and carbon and oxygen stable isotopes. As an example, different zones of a 40 μm size grain range in $\delta^{18}O$ from 37.1 ‰ to 24.9 ‰ and in $\Delta^{17}O$ from −3.0 ‰ to −1.3 ‰; the latter is similar to the total range in $\Delta^{17}O$ recorded in the present study (−2.57 ‰ and −0.96 ‰). Thus, over time the fluids from which Y 791198 type 1 calcite precipitated evolved isotopically, and possibly also became hotter; implicit in these observations is that the rate of calcite crystal growth was slower than the rate at which the fluid evolved. As type 1 calcite grains in other CMs show also oscillatory CL zoning (Brearley, 2006; Lee and Ellen, 2008; Lee et al., 2014; Telus et al., 2019), the processes recorded by Y-791198 were probably widespread within the CM parent body(ies). This initial phase of carbonate mineralization is summarised in Fig. 9**a**.

Precipitation of type 1 calcite was followed by growth of TCIs, which commonly surround and partially replace such carbonates (Lee et al., 2013,2014; Vacher et al., 2017) (Fig. 9**b**). By contrast, grains of type 2 calcite are not associated with TCIs indicating that they formed later, and this relative timing is consistent with their lower $\Delta^{17}O$ and $\delta^{18}O$ relative to type 1 (i.e., type 2 calcite precipitated from water that was more isotopically evolved, and maybe also hotter) (Tyra et al., 2012; Lee et al., 2013; Vacher et al., 2017,2018). As the abundance of aragonite in CMs falls with progressive aqueous alteration of the host meteorite (Lee et al., 2014), some of the early formed carbonates were dissolved or replaced by phyllosilicate as alteration progressed, and the ions liberated could have contributed to form other carbonates (Fig. 9**b**).

Data from the present study show that dolomite in SCO 06043 and ALH 83100 yield a lower $\Delta^{17}O$ and higher temperature than coexisting calcite, which would be consistent with dolomite precipitating after calcite as the system continued to evolve isotopically and heat up. Crystallization of dolomite at high temperatures (i.e., ~100 °C) suggests that a kinetic inhibition to dolomite crystal growth had been overcome (e.g., hydration of Mg ions, Lippmann, 1973). A caveat to the assumption that dolomite postdated calcite is that our calcite data will be an average of the isotopic compositions of multiple generations where present. For example, if a sample contained scarce grains of calcite that formed after dolomite, their isotopic signal could be swamped by more abundant early formed calcite. This possibility can be tested in ALH 83100, whose calcite and dolomite were analysed by Telus et al. (2019) using NanoSIMS. They obtained 12 analyses of calcite and 11 of dolomite. Ten of the calcite analyses have a higher $\delta^{18}O$ than the dolomite, which is consistent with earlier precipitation of calcite, although the two minerals have the same $\Delta^{17}O$ within error (note that here we use their matrix corrected dolomite data) (Telus et al., 2019). In-situ oxygen isotope data are also available for coexisting calcite and dolomite in Boriskino (CM2) (Verdier-Paoletti et al., 2019). On a three-isotope plot the 29 analyses of Boriskino calcite form two clusters that differ in $\delta^{18}O$ (average 34.0 ± 2.6 ‰ and 18.8 ± 1.7 ‰) and $\Delta^{17}O$ (average −0.8 ± 0.5 ‰ and −2.5 ± 0.8 ‰). Five dolomite analyses plot in a third cluster with a lower $\delta^{18}O$ than all but one of the calcite analyses (average 14.7 ± 2.0 ‰), again implying that the dolomite grew later from hotter and/or more evolved fluids. In common with ALH 83100, $\Delta^{17}O$ of dolomite and calcite in Boriskino are indistinguishable within error (average of dolomite = -3.0 ± 0.8 ‰; average of the low $\delta^{18}O$ calcite cluster = -2.5 ± 0.8 ‰) (Verdier-Paoletti et al., 2019).

Although the in-situ data support a calcite-to-dolomite paragenesis, petrographic relationships between the two minerals where they are intergrown are often ambiguous (e.g., Fig. 1**f**). Lee et al. (2014) interpreted some of the calcite in highly aqueously altered CMs including ALH 83100 and SCO 06043 to have replaced dolomite. Overall, the in-situ isotopic data and petrographic observations discussed above indicate that calcite crystals in any one sample grew as the aqueous system was evolving isotopically and thermally, and in samples where the two minerals occur together, most of the calcite formed before dolomite.

5.5.2. *A time–temperature profile for parent body evolution*

The temperatures at which calcite and dolomite crystals grew can be used to help constrain the time–temperature evolution of a CM parent body. From ^{53}Mn-^{53}Cr ages of CM carbonates, Fujiya et al. (2012) constructed models for the thermal evolution of an asteroid 30 km in radius. They assumed that the body was primarily heated by the decay of ^{26}Al, and there was no fluid flow (i.e., the closed system model of Clayton and Mayeda, 1999). Two of the meteorites whose carbonates they dated were also analysed in the present study and they span the entire range of clumped isotope temperatures: Murchison calcite (age = 4562.6 +1.4/−1.9 Myr, temperature from the present study = 5–22 °C) and ALH 83100 dolomite (age = 4562.8 +0.8/−1.0 Myr, temperature from the present study = 101 ± 16 °C). Thus, there is no resolvable difference in age of carbonates that formed at the temperature extremes identified in our study, thus constraining the rate of parent body heating. Fujiya et al. (2012) also analysed Y 791,198 calcite and Sayama dolomite, and using data from all four meteorites they calculated a weighted average age for carbonate formation of 4,563.4 +0.4/–0.5 Myr.

Using their thermal models, Fujiya et al. (2012) concluded that carbonate ages are consistent with parent body accretion ~3.5 myr after CAIs (Fig. 10). A section of thee thermal model is reproduced in Fig. 10. It indicates that temperatures consistent with calcite in Murchison would have been reached at shallow depths (e.g., 10 km beneath the surface). However, the carbonates in most other meteorites would have formed at greater depths, and the profile for 27 km beneath the surface is consistent with a prograde reaction and calcite precipitating before dolomite (e.g., as in ALH 83100).

5.5.3. *Relationship between carbonate isotopic composition and degree of alteration*

Here we seek to understand why the degree of aqueous alteration of our meteorite samples correlates with the temperatures at which their carbonates precipitated. This is not a trivial question because most of the studied CMs have been only partially aqueously altered and so some process acted to arrest water/rock interaction before it had gone to its largest possible extent. Most estimates of Water/Rock ratios are between

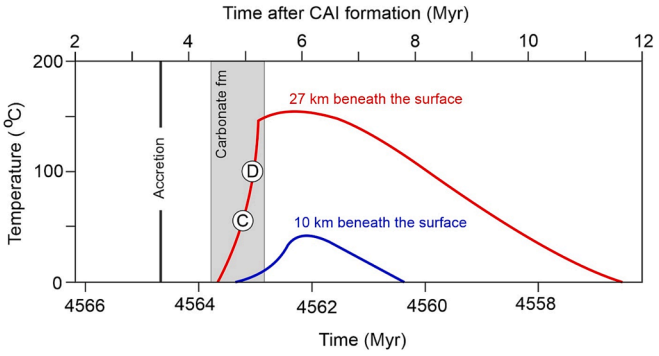

Fig. 10. Sections of the model in Fujiya et al. (2012) for heating of a 60 km diameter asteroid that accreted 3.5 myr after CAIs. The two solid lines are thermal profiles at 10 km beneath the asteroid's surface (blue) and at 27 km (red). C and D show where and when calcite and dolomite in ALH 83100 could have precipitated.

0.2 and 0.7 (Clayton and Mayeda, 1984 and, 1999, Verdier-Paoletti et al., 2019, Suttle et al., 2021 and references therein). One explanation is that parts of the parent body with high water/rock ratios were highly aqueously altered, and high temperatures were generated by exothermic serpentinization; areas with low water/rock ratios were less altered and corresponding cooler. However, if the amount of fluid was the limiting factor to the formation of alteration phases, we may expect to see variations in oxygen isotopic compositions of the last carbonate minerals reflecting a Rayleigh fractionation process.

A second possible reason for the correlation between carbonate temperature and degree of alteration is that water/rock interaction was 'switched off' in all parent body regions simultaneously. The switch could have been physical disruption of the parent body leading to a phase change, for example liquid water to ice following large scale fragmentation and rapid cooling, or liquid water to gas accompanying fracturing and depressurisation. At the time of this event, cooler and shallower parent body regions had been mildly altered, whereas hotter and deeper regions had been more highly altered because reactions had proceeded more quickly (i.e., water/rock ratio and the duration of aqueous alteration were similar, but reaction rate varied with depth and temperature). The agent of disruption could have been an impact, or overpressure due to the build-up of gases (e.g., H_2, CH_4) released by aqueous alteration (Wilson et al., 1999).

A third explanation for the correlation between carbonate temperature and degree of alteration is that a hydrothermal system was active in the CM meteorite parent body(ies). The highly aqueously altered meteorites were sourced from regions that were exposed to hot fluids whereas the mildly altered ones were from regions where aqueous fluids were cooler. If the hydrothermal system operated for the same duration in all regions, parts that were exposed to the hotter fluids would have been more altered owing to higher reaction rates. However, a problem with this model is that the hot (up-flow) fluids might be expected to be less isotopically evolved (i.e., higher $\Delta^{17}O$) than the cooler (down-flow) fluids, which had been reacting with anhydrous silicates for longer, which contradicts our isotope data.

A variant of the hydrothermal model is that all meteorites analysed here had a similar early evolution (Fig. 9**a, b**), but a subset were exposed to a pulse of hot and isotopically evolved fluids that were introduced by fractures (Fig. 9**c**). The new generation of fluids precipitated calcite and/or dolomite, and enhanced aqueous alteration of the host rocks. This model is consistent with evidence for fracture-mediated fluid flow in those meteorites used in the present study that are more highly altered. Specifically, Lee et al. (2013) described a millimetre size vein in LON 94101 whose calcite had considerably lower $\delta^{18}O$ and $\Delta^{17}O$ values than grains of aragonite and type 1 calcite elsewhere in the same thin section. The vein calcite was interpreted to have been precipitated from fluids of a low $\delta^{18}O$/high temperature and a low $\Delta^{17}O$ that had been introduced from elsewhere in the parent body via impact-formed fractures. Calcite veins have also been described from Cold Bokkeveld (Barber, 1981; Benedix et al., 2003), and dolomite veins occur in the two most highly altered meteorites analysed in the present study, SCO 06043 (Lee et al., 2014; Fig. 1**e**) and ALH 84051, which is paired with ALH 83100 (Tyra et al., 2010). This model is consistent with a study of Boriskino by Vacher et al. (2018), which revealed a close link between shock deformation and the isotopic composition of carbonates; their type 2 calcite formed from evolved ^{16}O-rich fluids that had been introduced via fractures. We conclude that our clumped isotope data are best explained by a two-step model of parent body aqueous alteration whereby all of the samples had a similar initial evolution (i.e., Fig. 9**a and b**) and some including ALH 83100 and SCO 06043 were exposed to a late pulse of hot and isotopically evolved fluids that were introduced via shock-formed fractures and precipitated dolomite and possibly also some calcite (Fig. 9**c**).

6. Conclusions

We have reported carbon, triple oxygen and clumped isotope compositions of carbonate minerals for six CM chondrites representing a range of degrees of aqueous alteration. We used a bulk extraction method (acid digestion) that allowed for separate extraction of calcite and dolomite where both minerals were present. We have analyzed the $\Delta^{17}O$ and Δ_{47} from the same aliquots of CO_2 to avoid potential biases due to the brecciated nature of CM chondrites and variability between splits. Our conclusions can be summarized as follows:

- Our carbon and oxygen isotope compositions are in good agreement with previous studies on the analyzed CM chondrites and fit within the general trend described by Alexander al. (2015). A notable exception is that we did not observe elevated $\delta^{13}C$ values that led Guo and Eiler (2007) to suggest methane generation.
- Our $\Delta^{17}O$ data is in good agreement with the study of Benedix et al. (2003). In situ studies show greater dispersion (Table 3) but have larger uncertainties which make comparisons more difficult.
- Based on clumped isotopic composition, we report temperatures of formation of 5 to 51 °C for calcite and 75 to 101 °C for dolomite in our samples (Table 2). As shown by in situ studies, carbonate minerals in CM chondrites display a range of carbon and oxygen isotopic compositions, and presumably a range in formation temperatures. Because we used a bulk extraction method, reported values are the weighted average for a carbonate phase in each sample. Although this has the potential to bias calculated temperatures, we show that the magnitude of the potential offset is similar to our measurement precision.
- We also report the oxygen isotopic composition of the fluids in equilibrium with the carbonates. We find that their $\delta^{18}O_{VSMOW}$ ranges from −6.6 to +2.3 ‰. There is no strong relationship between the $\delta^{18}O$ of the fluid with the $\delta^{13}C$ of the carbonates or with the formation temperature, which precludes the existence of a single starting fluid common to all samples in this study.
- The overall trend of our data is that CM chondrites that are more altered have carbonates with lower $\Delta^{17}O$ and higher formation temperatures (Figs. 3 and 4). It is consistent with dolomite forming after calcite in our samples. We present a qualitative model for the formation of carbonate minerals in CM chondrites, showing our data are consistent with a prograde reaction in a system that was largely closed, although hot and isotopically evolved fluids could have been introduced from other parent body regions in the latter stages of aqueous alteration.

Data availability

Research data has been supplied via a repository: https://doi.org/10.17632/49xtg98wz3.1.

CRediT authorship contribution statement

Matthieu Clog: Investigation, Validation, Visualization, Writing – original draft, Writing – review & editing. **Paula Lindgren:** Conceptualization, Resources, Validation, Writing – original draft, Writing – review & editing. **Sevasti Modestou:** Investigation, Validation, Writing – review & editing. **Alex McDonald:** Investigation, Validation. **Andrew Tait:** Investigation, Validation. **Terry Donnelly:** Investigation, Validation. **Darren Mark:** Funding acquisition, Writing – review & editing. **Martin Lee:** Conceptualization, Funding acquisition, Resources, Writing – original draft, Writing – review & editing.

Declaration of competing interest

The authors declare that they have no known competing financial interests or personal relationships that could have appeared to influence

the work reported in this paper.

Acknowledgements

We thank the Natural History Museum, London, and ANSMET for the loan of samples. US Antarctic meteorite samples are recovered by the Antarctic Search for Meteorites (ANSMET) program, which has been funded by NSF and NASA, and characterized and curated by the Department of Mineral Sciences of the Smithsonian Institution and Astromaterials Acquisition and Curation Office at NASA Johnson Space Center.

We acknowledge funding from the UK Science and Technology Facilities Council (STFC) through grants ST/W001128/1, ST/T002328/1, ST/G001693/1 and ST/K000942/1.

Appendix A. Supplementary material

There are three supplementary files attached to this article. The first one describes in more detail the validation of the analytical methods used in this paper and the data processing workflow. The second file is a spreadsheet with the data for the clumped isotope measurements of each reference material and meteorite replicate analyzed in this study. The third is a spreadsheet with the data for the triple oxygen isotope composition measurements for each meteorite replicate and the results of the validation measurements on terrestrial carbonates. Supplementary material to this article can be found online at https://doi.org/10.1016/j.gca.2024.01.023.

References

Adnew, G.A., Hofmann, M.E., Paul, D., Laskar, A., Surma, J., Albrecht, N., Pack, A., Schwieters, J., Koren, G., Peters, W., Röckmann, T., 2019. Determination of the triple oxygen and carbon isotopic composition of CO_2 from atomic ion fragments formed in the ion source of the 253 Ultra high-resolution isotope ratio mass spectrometer. Rapid Commun. Mass Spectrom. 33 (17), 1363–1380.

Alexander, C.M.O'D., Bowden, R., Fogel, M.L., Howard, K.T., Herd, C.D.K., Nittler, L.R., 2012. The provenances of asteroids, and their contributions to the volatile inventories of the terrestrial planets. Science 337, 721–723.

Alexander, C.M.O'D., Howard, K.T., Bowden, R., Fogel, M.L., 2013. The classification of CM and CR chondrites using bulk H, C and N abundances and isotopic compositions. Geochim. Cosmochim. Acta 123, 244–260.

Alexander, C.M.O'D., Bowden, R., Fogel, M.L., Howard, K.T., 2015. Carbonate abundances and isotopic compositions in chondrites. Meteorit. Planet. Sci. 50, 810–833.

Amsellem, E., Moynier, F., Mahan, B., Beck, P., 2020. Timing of thermal metamorphism in CM chondrites: Implications for Ryugu and Bennu future sample return. Icarus 339, 113593.

Anderson, F.W., Dunham K.C., 1966. The Geology of Northern Skye. Memoirs of the Geological Survey of Great Britain. Her Majesty's stationery office, Edinburgh.

Anderson, N.T., Kelson, J.R., Kele, S., Daëron, M., Bonifacie, M., Horita, J., Mackey, T.J., John, C.M., Kluge, T., Petschnig, P., Jost, A.B., Huntington, K.W., Bernasconi, S.M., Bergmann, K.D., 2021. A unified clumped isotope thermometer calibration (0.5–1,100 C) using carbonate-based standardization. Geophys. Res. Lett. 48 (7), e2020GL092069.

Barber, D.J., 1981. Matrix phyllosilicates and associated minerals in C2M carbonaceous chondrites. Geochim. Cosmochim. Acta 45, 945–970.

Benedix, G.K., Leshin, L.A., Farquhar, J., Jackson, T., Thiemens, M.H., 2003. Carbonates in CM2 chondrites: Constraints on alteration conditions from oxygen isotopic compositions and petrographic observations. Geochim. Cosmochim. Acta 67 (8), 1577–1588.

Bernasconi, S.M., Daëron, M., Bergmann, K.D., Bonifacie, M., Meckler, A.N., Affek, H.P., Anderson N., Bajnai D., Barkan E., Beverly E., Blamart D., Burgener, L., Calmels, D., Chaduteau, C., Clog, M., Davidheiser-Kroll, B., Davies, A., Dux, F., Eiler, J., Elliott, B., Fetrow, A.C., Fiebig, J., Goldberg, S., Hermoso, M., Kuntington, K.W., Hyland, E., Ingalls, M., Jaggi, M., John, C.M., Jost, A.B., Katz, S., Kelson. J., Kluge, T., Kocken, I. J., Laskar, A., Leutert, T.J., Liang, D., Lucarelli, J., Mackey, T.J., Mangenot, X., Meinicke, N., Modestou, S.E., Müller, I.A., Murray, S., Neary, A., Packard, N., Passey, B.H., Pelletier, E., Petersen, S., Piasecki, A., Schauer, A., Snell, K.E., Swart, P.K., Tripati, A., Upadhyay, D., Vennemann, T., Winkelstern, I., Yarian, D., Yoshida, N., Zhang, N., Ziegler, M., 2021. InterCarb: A community effort to improve interlaboratory standardization of the carbonate clumped isotope thermometer using carbonate standards. Geochem. Geophys. Geosyst., 22(5), e2020GC009588.

Bischoff, A., Scott, E.R., Metzler, K., Goodrich, C.A., 2006. Nature and origins of meteoritic breccias. Meteorites and the early solar system II 679–712.

Borovička, J., Popova, O., Spurný, P., 2019. The Maribo CM 2 meteorite fall—Survival of weak material at high entry speed. Meteorit. Planet. Sci. 54 (5), 1024–1041.

Brand, W.A., Assonov, S.S., Coplen, T.B., 2010. Correction for the ^{17}O interference in $\delta(^{13}C)$ measurements when analyzing CO_2 with stable isotope mass spectrometry (IUPAC Technical Report). Pure Appl. Chem. 82 (8), 1719–1733.

Brearley, A.J., 2006. The action of water. In: Lauretta, D.S., McSween Jr., H. Y. (Eds.) Meteorites and the Early Solar System II. University of Arizona Press, pp. 587–624.

Bunch, T.E., Chang, S., 1980. Carbonaceous chondrites – II. Carbonaceous chondrite phyllosilicates and light element geochemistry as indicators of parent body processes and surface conditions. Geochimica Cosmochimica Acta 44, 1543–1577.

Burbine, T.H., 2016. Advances in determining asteroid chemistries and mineralogies. Geochemistry 76 (2), 181–195.

Clayton, R.N., Mayeda, T.K., Rubin, A.E., 1984. Oxygen isotopic compositions of enstatite chondrites and aubrites. J. Geophys. Res.: Solid Earth 89 (S01), C245–C249.

Clayton, R.N., Mayeda, T.K., 1999. Oxygen isotope studies of carbonaceous chondrites. Geochim. Cosmochim. Acta 63, 2089–2104.

Connolly Jr., H.C., Smith, C., Benedix, G., Folco, L., Righter, K., Zipfel, J., Yamaguchi, A., Chennaoui Aoudjehane, H., 2007. The Meteoritical Bulletin, No. 92, 2007 September. Meteorit. Planet. Sci. 42, 1647–1694.

Daëron, M., 2021. Full propagation of analytical uncertainties in Δ_{47} measurements. Geochem. Geophys. Geosyst. 22 (5), e2020GC009592.

De Leuw, S., Rubin, A.E., Schmidt, A.K., Wasson, J.T., 2010. Carbonates in CM chondrites: complex formational histories and comparison to carbonates in CI chondrites. Meteorit. Planet. Sci. 45, 513–530.

Defliese, W.F., Lohmann, K.C., 2015. Non-linear mixing effects on mass-47 CO_2 clumped isotope thermometry: Patterns and implications. Rapid Commun. Mass Spectrom. 29 (9), 901–909.

DuFresne, E.R., Anders, E., 1962. On the chemical evolution of the carbonaceous chondrites. Geochim. Cosmochim. Acta 26 (11), 1085–1114.

Eiler, J.M., Schauble, E., 2004. $^{18}O^{13}C^{16}O$ in Earth's atmosphere. Geochim. Cosmochim. Acta 68 (23), 4767–4777.

Farsang, S., Franchi, I.A., Zhao, X., Raub, T.D., Redfern, S.A.T., Grady, M.M., 2021. Carbonate assemblages in Cold Bokkeveld CM chondrite reveal complex parent body evolution. Meteorit. Planet. Sci. 56, 723–741.

Fuchs, L. H., Olsen, E., Jensen, K.J., 1973. Mineralogy, mineral-chemistry, and composition of the Murchison (C2) meteorite. Smithsonian Contributions to the Earth Sciences.

Fujiya, W., Sugiura, N., Hotta, H., Ichimura, K., Sano, Y., 2012. Evidence for the late formation of hydrous asteroids from young meteoritic carbonates. Nat. Commun. 3 (1), 627.

Fujiya, W., Sugiura, N., Marrocchi, Y., Takahata, N., Hoppe, P., Shirai, K., Sano, Y., Hiyagon, H., 2015. Comprehensive study of carbon and oxygen isotopic compositions, trace element abundances, and cathodoluminescence intensities of calcite in the Murchison CM chondrite. Geochim. Cosmochim. Acta 161, 101–117.

Fujiya, W., Aoki, Y., Ushikubo, T., Hashizume, K., Yamaguchi, A., 2020. Carbon isotopic evolution of aqueous fluids in CM chondrites: clues from in-situ isotope analyses within calcite grains in Yamato-791198. Geochim. Cosmochim. Acta 274, 246–260.

Fujiya, W., Higashi, H., Hibiya, Y., Sugawara, S., Yamaguchi, A., Kimura, M., Hashizume, K., 2022. Hydrothermal activities on C-complex asteroids induced by radioactivity. The Astrophysical Journal Letters 924 (1), L16.

Gradie, J., Tedesco, E., 1982. Compositional structure of the asteroid belt. Science 216 (4553), 1405–1407.

Grady, M.M., Wright, I.P., Swart, P.K., Pillinger, C.T., 1988. The carbon and oxygen isotopic composition of meteoritic carbonates. Geochim. Cosmochim. Acta 52 (12), 2855–2866.

Graham, A.L., Bevan, A.W.R., Hutchison, R., 1985 Catalogue of Meteorites: with special reference to those represented in the collection of the British Museum (Natural History), fourth ed. 460p.

Greenwood, R.C., Lee, M.R., Hutchison, R., Barber, D.J., 1994. Formation and alteration of CAIs in Cold Bokkeveld (CM2). Geochim. Cosmochim. Acta 58, 1913–1935.

Greenwood, R.C., Burbine, T.H., Franchi, I.A., 2020. Linking asteroids and meteorites to the primordial planetesimal population. Geochim. Cosmochim. Acta 277, 377–406.

Grimm, R.E., McSween Jr, H.Y., 1989. Water and the thermal evolution of carbonaceous chondrite parent bodies. Icarus 82 (2), 244–280.

Grossman, J.N., 1994. The Meteoritical Bulletin, No. 76, 1994 January: the US Antarctic meteorite collection. Meteoritics 29, 100–143.

Grossman, J.N., Score, R., 1996. The Meteoritical Bulletin, No. 79, 1996 July: recently classified specimens in the United States meteorite collection. Meteoritics Planet. Sci. 31, A161–A174.

Guo, W., Eiler, J.M., 2007. Temperatures of aqueous alteration and evidence for methane generation on the parent bodies of the CM chondrites. Geochim. Cosmochim. Acta 71 (22), 5565–5575.

Hemingway, J.D., Henkes, G.A., 2021. A disordered kinetic model for clumped isotope bond reordering in carbonates. Earth Planet. Sci. Lett. 566, 116962.

Howard, K.T., Benedix, G.K., Bland, P.A., Cressey, G., 2009. Modal mineralogy of CM2 chondrites by X-ray diffraction (PSD-XRD). Part 1: total phyllosilicate abundance and the degree of aqueous alteration. Geochim. Cosmochim. Acta 73, 4576–4589.

Howard, K.T., Benedix, G.K., Bland, P.A., Cressey, G., 2011. Modal mineralogy of CM chondrites by X-ray diffraction (PSD-XRD). Part 2: degree, nature and settings of aqueous alteration. Geochim. Cosmochim. Acta 75, 2735–2751.

Howard, K.T., Alexander, C.M.O'.D., Schrader, D.L., Dyl, K.A., 2015. Classification of hydrous meteorites (CR, CM and C2 ungrouped) by phyllosilicate fraction: PSD-XRD

modal mineralogy and planetesimal environments. Geochim. Cosmochim. Acta 149, 206–222.
Jenniskens, P., Fries, M., Yin, Q.Z., Zolensky, M., Krot, A.N., Sandford, S.A., Sears, D., Beauford, R., Ebel, D.S., Friedrich, J.M., Nagashima, K., Wimpenny, J., Yamakawa, A., Nishiizumi, K., Hamajima, Y., Caffee, M.W., Welten, K.C., Laubenstein, M., Davis, A.N., Simon, S.B., Heck, P.R., Young, E.D., Kohl, I.E., Thiemens, M.H., Nunn, M.H., Mikouchi, T., Hagiya, K., Ohsumi, K., Cahill, T.A., Lawton, J.A., Barnes, D., Steele, A,, Rochette, P., Verosub, K.L., Gattacceca, J., Cooper, G., Glavin, D.P., Burton, A.S., Dworkin, J.P., Elsila, J.E., Pizzarello, S., Ogliore, R., Schmitt-Kopplin, P., Harir, M., Hertkorn, N., Verchovsky, A., Grady, M., Nagao, K., Okazaki, R., Takechi, H., Hiroi, T., Smith, K., Silber, E.A., Brown, P.G., Albers, J., Klotz, D., Hankey, M., Matson, R., Fries, J.A., Walker, R.J., Puchtel, I., Lee, C.T.A., Erdman, M.E., Eppich, G.R., Roeske, S., Gabelica, Z., Lerche, M., Nuevo, M., Girten, B., Worden, S.P., and (the Sutter's Mill Meteorite Consortium), 2012. Radar-enabled recovery of the Sutter's Mill meteorite, a carbonaceous chondrite regolith breccia. Science, 338(6114), 1583–1587.
John, C.M., Bowen, D., 2016. Community software for challenging isotope analysis: first applications of 'Easotope' to clumped isotopes. Rapid Commun. Mass Spectrom. 30 (21), 2285–2300.
Johnson, C.A., Prinz, M., 1993. Carbonate compositions in CM and CI chondrites, and implications for aqueous alteration. Geochim. Cosmochim. Acta 57, 2843–2852.
Kim, S.T., Mucci, A., Taylor, B.E., 2007. Phosphoric acid fractionation factors for calcite and aragonite between 25 and 75 C: revisited. Chem. Geol. 246 (3–4), 135–146.
King, A.J., Schofield, P.F., Russell, S.S., 2017. Type 1 aqueous alteration in CM carbonaceous chondrites: Implications for the evolution of water-rich asteroids. Meteorit. Planet. Sci. 52 (6), 1197–1215.
King, A.J., Daly, L., Rowe, J., Joy, K.H., Greenwood, R.C., Devillepoix, H.A.R., Suttle, M. D., Chan, Q.H.S., Russell, S.S., Bates, H.C., Bryson, J.F.J., Clay, P.L., Vida, D., Lee, M. R., O'Brien, Á., Hallis, L.J., Natasha, R., Stephen, R.T., Sansom, E.K., Towner, M.C., Cupak, M., Shober, P.M., Bland, P.A., Findlay, R., Franchi, I.A., Verchovsky, A.B., Abernethy, F.A.J., Grady, M.M., Floyd, C.J., Van Ginneken, M., Bridges, J., Hicks, L. J., Jones, R.H., Mitchell, J.T., Genge, M.J., Jenkins, L., Martin, P.-E., Sephton, M.A., Watson, J.S., Salge, T., Shirley, K.A., Curtis, R.J., Warren, T.J., Bowles, N.E., Stuart, F.M., Di Nicola, L., Györe, D., Boyce, A.J., Shaw, K.M.M., Elliott, T., Steele, R. C.J., Povinec, P., Laubenstein, M., Sanderson, D., Cresswell, A., Jull, A.J.T., Sýkora, I., Sridhar, S., Richard, J., Harrison,, Willcocks, F.M., Harrison, C.S., Hallatt, D., Wozniakiewicz, P.J., Burchell, M.J., Luke Alesbrook, S., Dignam, A., Almeida, N.V., Smith, C.L., Clark, B., Humphreys-Williams, E.R., Schofield, P.F., Cornwell, L.T., Spathis, V., Morgan, G.H., Perkins, M.J., Kacerek, R., Campbell-Burns, P., Colas, F., Zanda, B., Vernazza, P., Bouley, S., Jeanne, S., Hankey, M., Collins, G.S., Young, J.S., Shaw, C., Horak, J., Jones, D., James, N., Bosley, S., Shuttleworth, A., Dickinson, P., McMullan, I., Robson, D., Smedley, A.R.D., Stanley, B., Bassom, R., McIntyre, M., Suttle, A.A., Fleet, R., Bastiaens, L., Ihász, Míra.B., McMullan, S., Boazman, S.J., Dickeson, Z.I., Grindrod, P.M., Pickersgill, A.E., Weir, C.J., Suttle, F.M., Farrelly, S., Spencer, I., Naqvi, S., Mayne, B., Skilton, D., Kirk, D., Mounsey, A., Mounsey, S.E., Mounsey, S., Godfrey, P., Bond, L., Bond, V., Wilcock, C., Wilcock, H., Wilcock, R., 2022. The Winchcombe meteorite, a unique and pristine witness from the outer solar system. Sci. Adv. 8 (46), eabq3925.
Le Guillou, C., Zanetta, P., Leroux, H., Brearley, A., Zanda, B., Hewins, R., 2019. Amorphous Silicates in Carbonaceous and Ordinary Chondrites. In: 82nd Annual Meeting of The Meteoritical Society, vol. 82, No. 2157, p. 6267.
Lee, M.R., 1993. The petrography, mineralogy and origins of calcium sulphate within the Cold Bokkeveld CM carbonaceous chondrite. Meteoritics 28, 53–62.
Lee, M.R., Ellen, R., 2008. Aragonite in the Murray (CM2) carbonaceous chondrite: implications for parent body compaction and aqueous alteration. Meteorit. Planet. Sci. 43 (7), 1219–1231.
Lee, M.R., Daly, L., Floyd, C., Martin, P.-E., 2021a. CM carbonaceous chondrite falls and their terrestrial alteration. Meteorit. Planet. Sci. 56, 34–48.
Lee, M.R., Cohen, B.E., Boyce, A.J., Hallis, L.J., Daly, L., 2021b. The pre-atmospheric hydrogen inventory of CM carbonaceous chondrites. Geochim. Cosmochim. Acta 309, 31–44.
Lee, M.R., Floyd, C., Martin, P.E., Zhao, X., Franchi, I.A., Jenkins, L., Griffin, S., 2023a. Extended time scales of carbonaceous chondrite aqueous alteration evidenced by a xenolith in L a P az Icefield 02239 (CM2). Meteorit. Planet. Sci.
Lee, M.R., Sofe, M.R., Lindgren, P., Starkey, N.A., Franchi, I.A., 2013. The oxygen isotope evolution of parent body aqueous solutions as recorded by multiple carbonate generations in the Lonewolf Nunataks 94101 CM2 carbonaceous chondrite. Geochim. Cosmochim. Acta 121, 452–466.
Lee, M.R., Lindgren, P., Sofe, M.R., 2014. Aragonite, breunnerite, calcite and dolomite in the CM carbonaceous chondrites: high fidelity recorders of progressive parent body aqueous alteration. Geochim. Cosmochim. Acta 144, 126–156.
Lee, M.R., Lindgren, P., King, A.J., Greenwood, R.C., Franchi, I.A., Sparkes, R., 2016. Elephant Moraine 96029, a very mildly aqueously altered and heated CM carbonaceous chondrite: implications for the drivers of parent body processing. Geochim. Cosmochim. Acta 92, 148–169.
Lee, M.R., Hallis, L.J., Daly, L., Boyce, A.J., 2023b. The water content of CM carbonaceous chondrite falls and finds, and their susceptibility to terrestrial contamination. Meteorit. Planetary Sci. 58 (12), 1760–1772.
Lentfort, S., Bischoff, A., Ebert, S., Patzek, M., 2020. Classification of CM chondrite breccias—Implications for the evaluation of samples from the OSIRIS-Rex and Hayabusa 2 missions. Meteorit. Planet. Sci. 56, 127–147.
Lindgren, P., Lee, M.R., Sofe, M., Burchell, M.J., 2011. Microstructure of calcite in the CM2 carbonaceous chondrite LON 94101: Implications for deformation history during and/or after aqueous alteration. Earth Planet. Sci. Lett. 306, 289–298.
Lindgren, P., Lee, M.R., Sofe, M.R., Zolensky, M.E., 2013. Clasts in the CM2 carbonaceous chondrite Lonewolf Nunataks 94101: evidence for aqueous alteration prior to complex mixing. Meteorit. Planet. Sci. 48, 1074–1090.
Lindgren, P., Hanna, R.D., Dobson, K.J., Tomkinson, T., Lee, M.R., 2015. The paradox between low shock-stage and evidence for compaction in CM carbonaceous chondrites explained by multiple low-intensity impacts. Geochim. Cosmochim. Acta 148, 159–178.
Lindgren, P., Lee, M.R., Starkey, N.A., Franchi, I.A., 2017. Fluid evolution in CM carbonaceous chondrites tracked through the oxygen isotopic compositions of carbonates. Geochim. Cosmochim. Acta 204, 240–251.
Lindgren, P., Lee, M.R., Sparkes, R., Lindgren, P., Lee, M.R., Sparkes, R., Greenwood, R. C., Hanna, R.D., Franchi, I.A., King, A.J., Floyd, C., Martin, P.E., Hamilton, V.E., Haberle, C., 2020. Signatures of the post-hydration heating of highly aqueously altered CM carbonaceous chondrites and implications for interpreting asteroid sample returns. Geochim. Cosmochim. Acta 289, 69–92.
Lippmann, F., 1973 Sedimentary carbonate minerals. In: Minerals, Rocks and Inorganic Materials, Monograph Series of Theoretical and Experimental Studies, vol. 6. Springer, Berlin, p. 228.
Lloyd, M.K., Eiler, J.M., Nabelek, P.I., 2017. Clumped isotope thermometry of calcite and dolomite in a contact metamorphic environment. Geochim. Cosmochim. Acta 197, 323–344.
Mackinnon, I.D., Zolensky, M.E., 1984. Proposed structures for poorly characterized phases in C2M carbonaceous chondrite meteorites. Nature 309 (5965), 240–242.
Nakamura, T., 2005. Post-hydration thermal metamorphism of carbonaceous chondrites. J. Mineral. Petrol. Sci. 100 (6), 260–272.
Passey, B.H., Hu, H., Ji, H., Montanari, S., Li, S., Henkes, G.A., Levin, N.E., 2014. Triple oxygen isotopes in biogenic and sedimentary carbonates. Geochim. Cosmochim. Acta 141, 1–25.
Petersen, S.V., Defliese, W.F., Saenger, C., Daëron, M., Huntington, K.W., John, C.M., Kelson, J.R., Bernasconi, S.M., Colman, A.S., Kluge, T., Olack, G.A., Schauer, A.J., Bajnai, D., Bonifacie, M., Breitenbach, S.F.M., Fiebig, J., Fernandez, A.B., Henkes, G. A., Hodell, D., Katz, A., Kele, S., Lohmann, K.C., Passey, B.H., Peral, M.Y., Petrizzo, D.A., Rosenheim, B.E., Tripati, A., Venturelli, R., Young, E.D., Winkelstern, I.Z., 2019. Effects of improved ^{17}O correction on interlaboratory agreement in clumped isotope calibrations, estimates of mineral-specific offsets, and temperature dependence of acid digestion fractionation. Geochem. Geophys. Geosyst. 20 (7), 3495–3519.
Rosenbaum, J., Sheppard, S.M.F., 1986. An isotopic study of siderites, dolomites and ankerites at high temperatures. Geochim. Cosmochim. Acta 50 (6), 1147–1150.
Rubin, A.E., 2012. Collisional facilitation of aqueous alteration of CM and CV carbonaceous chondrites. Geochim. Cosmochim. Acta 90, 181–194.
Rubin, A.E., 2015. An American on Paris: Extent of aqueous alteration of a CM chondrite and the petrography of its refractory and amoeboid olivine inclusions. Meteorit. Planet. Sci. 50, 1595–1612.
Rubin, A.E., Trigo-Rodriguez, J.M., Huber, H., Wasson, J.T., 2007. Progressive aqueous alteration of CM carbonaceous chondrites. Geochim. Cosmochim. Acta 71, 2361–2382.
Singerling, S.A., Brearley, A.J., 2018. Primary iron sulfides in CM and CR carbonaceous chondrites: Insights into nebular processes. Meteorit. Planet. Sci. 53 (10), 2078–2106.
Singerling, S.A., Brearley, A.J., 2020. Altered primary iron sulfides in CM 2 and CR 2 carbonaceous chondrites: Insights into parent body processes. Meteorit. Planet. Sci. 55 (3), 496–523.
Stolper, D.A., Eiler, J.M., 2015. The kinetics of solid-state isotope-exchange reactions for clumped isotopes: A study of inorganic calcites and apatites from natural and experimental samples. Am. J. Sci. 315 (5), 363–411.
Suttle, M.D., King, A.J., Schofield, P.F., Bates, H., Russell, S.S., 2021. The aqueous alteration of CM chondrites, a review. Geochim. Cosmochim. Acta 299, 219–256.
Telus, M., Hauri, E.H., Wang, J., 2019. Calcite and dolomite formation in the CM parent body: Insight from in situ C and O isotope analyses. Geochim. Cosmochim. Acta 260, 275–291.
Tomeoka, K., McSween Jr, H.Y., Buseck, P.R., 1989. Mineralogical alteration of CM carbonaceous chondrites: a review. In: Proceedings of the NIPR symposium on antarctic meteorites, vol. 2, pp. 221–234.
Tonui, E., Zolensky, M., Hiroi, T., Nakamura, T., Lipschutz, M.E., Wang, M.S., Okudaira, K., 2014. Petrographic, chemical and spectroscopic evidence for thermal metamorphism in carbonaceous chondrites I: CI and CM chondrites. Geochim. Cosmochim. Acta 126, 284–306.
Tyra, M., Brearley, A., Guan, Y., 2016. Episodic carbonate precipitation in the CM chondrite ALH 84049: An ion microprobe analysis of O and C isotopes. Geochim. Cosmochim. Acta 175, 195–207.
Tyra, M.A., Matzel, J., Brearley, A.J., Hutcheon, I.D., 2010. Variability in carbonate petrography and NanoSIMS $^{53}Mn/^{53}Cr$ systematics in paired CM1 chondrites ALH 84051, ALH 84049, and ALH 84034. Lunar Planet. Sci. XLI. Lunar Planet. Inst., Houston. #2687 (abstr).
Tyra, M.A., Farquhar, J., Guan, Y., Leshin, L.A., 2012. An oxygen isotope dichotomy in CM2 chondritic carbonates—A SIMS approach. Geochim. Cosmochim. Acta 77, 383–395.
Vacher, L.G., Marrocchi, Y., Villeneuve, J., Verdier-Paoletti, M.J., Gounelle, M., 2017. Petrographic and C & O isotopic characteristics of the earliest stages of aqueous alteration of CM chondrites. Geochim. Cosmochim. Acta 213, 271–290.
Vacher, L.G., Marrocchi, Y., Villeneuve, J., Verdier-Paoletti, M.J., Gounelle, M., 2018. Collisional and alteration history of the CM parent body. Geochim. Cosmochim. Acta 239, 213–234.
Vacher, L.G., Truche, L., Faure, F., Tissandier, L., Mosser-Ruck, R., Marrocchi, Y., 2019a. Deciphering the conditions of tochilinite and cronstedtite formation in CM

chondrites from low temperature hydrothermal experiments. Meteorit. Planet. Sci. 54 (8), 1870–1889.
Vacher, L.G., Piralla, M., Gounelle, M., Bizzarro, M., Marrocchi, Y., 2019b. Thermal evolution of hydrated asteroids inferred from oxygen isotopes. Astrophys. J. Lett. 882 (2), L20.
Vacher, L.G., Piani, L., Rigaudier, T., Thomassin, D., Florin, G., Piralla, M., Marrocchi, Y., 2020. Hydrogen in chondrites: Influence of parent body alteration and atmospheric contamination on primordial components. Geochim. Cosmochim. Acta 281, 53–66.
Verdier-Paoletti, M.J., Marrocchi, Y., Avice, G., Roskosz, M., Gurenko, A., Gounelle, M., 2017. Oxygen isotope constraints on the alteration temperatures of CM chondrites. Earth Planet. Sci. Lett. 458, 273–281.
Verdier-Paoletti, M.J., Marrocchi, Y., Vacher, L.G., Gattacceca, J., Gurenko, A., Sonzogni, C., Gounelle, M., 2019. Testing the genetic relationship between fluid alteration and brecciation in CM chondrites. Meteorit. Planet. Sci. 54, 1692–1709.
Visser, R., John, T., Whitehouse, M.J., Patzek, M., Bischoff, A., 2020. A short-lived 26Al induced hydrothermal alteration event in the outer solar system: constraints from Mn/Cr ages of carbonates. Earth Planet. Sci. Lett. 547, 116440.
Weisberg, M.K., Smith, C., Benedix, G., Folco, L., Righter, K., Zipfel, J., Yamaguchi, A., Chennaoui Aoudjehane, H., 2008. The Meteoritical Bulletin, No. 94, September 2008. Meteorit. Planet. Sci. 43, 1551–1588.
Wilson, L., Keil, K., Browning, L.B., Krot, A.N., Bourcier, W., 1999. Early aqueous alteration, explosive disruption, and reprocessing of asteroids. Meteorit. Planet. Sci. 34 (4), 541–557.
Yang, Y., Li, S., Zhu, M.H., Liu, Y., Wu, B., Du, J., Fa, W., Xu, R., He, Z., Wang, C., Xue, B., 2022. Impact remnants rich in carbonaceous chondrites detected on the Moon by the Chang'e-4 rover. Nat. Astronomy 6 (2), 207–213.
Zhang, A., Guan, Y., Hsu, W., Liu, Y., Taylor, L.A., 2010. Origin of a metamorphosed lithic clast in CM chondrite Grove Mountains 021536. Meteorit. Planet. Sci. 45 (2), 238–245.
Zolensky, M.E., Barrett, R., Browning, L., 1993. Mineralogy and composition of matrix and chondrule rims in carbonaceous chondrites. Geochim. Cosmochim. Acta 57 (13), 3123–3148.